September 11, 2011

Early Magnetic B-type Stars: X-ray Emission and Wind Properties.

L. M. Oskinova, *University of Potsdam*
H. Todt, *University of Potsdam*
Richard Ignace, *East Tennessee State University*
J. C. Brown, *University of Glasgow*
J. P. Cassinelli, *University of Wisconsin-Madison*, et al.

Monthly Notices
of the
ROYAL ASTRONOMICAL SOCIETY

Mon. Not. R. Astron. Soc. **416,** 1456–1474 (2011) doi:10.1111/j.1365-2966.2011.19143.x

Early magnetic B-type stars: X-ray emission and wind properties

L. M. Oskinova,[1⋆] H. Todt,[1] R. Ignace,[2] J. C. Brown,[3] J. P. Cassinelli[4] and W.-R. Hamann[1]

[1]*Institute for Physics and Astronomy, University of Potsdam, 14476 Potsdam, Germany*
[2]*Department of Physics and Astronomy, East Tennessee State University, Johnson City, TN 37614, USA*
[3]*School of Physics and Astronomy, University of Glasgow, Glasgow G12 8QQ*
[4]*Department of Astronomy, University of Wisconsin-Madison, Madison, WI 53711, USA*

Accepted 2011 May 27. Received 2011 May 27; in original form 2011 March 15

ABSTRACT

We present a comprehensive study of X-ray emission by, and wind properties of, massive magnetic early B-type stars. Dedicated *XMM–Newton* observations were obtained for three early-type B-type stars, ξ^1 CMa, V2052 Oph and ζ Cas, with recently discovered magnetic fields. We report the first detection of X-ray emission from V2052 Oph and ζ Cas. The latter is one the softest X-ray sources among the early-type stars, while the former is one of the X-ray faintest. The observations show that the X-ray spectra of our programme stars are quite soft with the bulk of X-ray emitting material having a temperature of about 1 MK. We compile the complete sample of early B-type stars with detected magnetic fields to date and existing X-ray measurements, in order to study whether the X-ray emission can be used as a general proxy for stellar magnetism. We find that the X-ray properties of early massive B-type magnetic stars are diverse, and that hard and strong X-ray emission does not necessarily correlate with the presence of a magnetic field, corroborating similar conclusions reached earlier for the classical chemically peculiar magnetic Bp–Ap stars.

We analyse the ultraviolet (UV) spectra of five non-supergiant B stars with magnetic fields (τ Sco, β Cep, ξ^1 CMa, V2052 Oph and ζ Cas) by means of non-local thermodynamic equilibrium (non-LTE) iron-blanketed model atmospheres. The latter are calculated with the Potsdam Wolf–Rayet (PoWR) code, which treats the photosphere as well as the wind, and also accounts for X-rays. With the exception of τ Sco, this is the first analysis of these stars by means of stellar wind models. Our models accurately fit the stellar photospheric spectra in the optical and the UV. The parameters of X-ray emission, temperature and flux are included in the model in accordance with observations. We confirm the earlier findings that the filling factors of X-ray emitting material are very high.

Our analysis reveals that the magnetic early-type B stars studied here have weak winds with velocities not significantly exceeding $v_{\rm esc}$. The mass-loss rates inferred from the analysis of UV lines are significantly lower than predicted by hydrodynamically consistent models. We find that, although the X-rays strongly affect the ionization structure of the wind, this effect is not sufficient in reducing the total radiative acceleration. When the X-rays are accounted for at the intensity and temperatures observed, there is still sufficient radiative acceleration to drive a stronger mass-loss than we empirically infer from the UV spectral lines.

Key words: techniques: spectroscopic – stars: magnetic field – stars: massive – stars: mass loss – X-rays: stars.

1 INTRODUCTION

Magnetic fields in massive stars ($M_* \gtrsim 8\,{\rm M}_\odot$) have the potential to influence stellar formation and evolution (e.g. Ferrario et al. 2009). Although discoveries of massive star magnetism are increasing (Hubrig et al. 2011; Petit et al. 2011), our knowledge of their existence, origin and the role they play remains limited. The routine presence of magnetic fields in these stars is observationally neither established nor disproved, due to the lack hitherto of suitable diagnostic tools and observations of adequate quality (for a recent review see Donati & Landstreet 2009). The

⋆E-mail: lida@astro.physik.uni-potsdam.de

Zeeman effect, commonly used to measure magnetic fields in solar-type stars, is less useful in hot stars: the line broadening by macroscopic motions exceeds the Zeeman splitting, unless the magnetic field is extremely strong.

While direct measurements of magnetic field have been possible only for the closest and brightest stars, there has been indirect evidence for magnetic fields on massive stars. The wide range of observational phenomena, such as ultraviolet (UV) wind-line periodic variability, cyclic variability in Hα and He II λ4686, and excess emission in UV wind lines centred about the rest wavelength (e.g. Henrichs, Schnerr & ten Kulve 2005; Schnerr et al. 2008) are commonly explained by the influence that magnetic fields exert on stellar winds. For example, cyclical wind line variability is likely due to a wind flow that is guided by a large-scale, dipole-like magnetic field corotating with the star. In these cases the time-scale of the variability is similar to the rotation period. Other indicators of magnetic fields may include chemical peculiarity, certain pulsation behaviour, non-thermal radio emission and anomalous X-ray emission.

In this paper we address the X-ray emission by and wind properties of magnetic B-type stars. Our study includes stars earlier than B2 that have both confirmed magnetic fields and X-ray data. Thus, our sample includes only massive stars, with initial masses exceeding $\sim$8 $M_{\odot}$. We consider the B-type stars, where magnetic fields have been detected only recently, as well as the earliest types of 'classical' chemically peculiar Bp-type stars. The latter have a high incidence of strong magnetic fields (e.g. Bychkov, Bychkova & Madej 2003). Much work has already been done to study the X-ray emission from chemically peculiar magnetic Bp and Ap stars. Using the results from X-ray surveys, correlations between the X-ray properties of these stars and their magnetism were investigated by Drake et al. (1994) and Leone (1994). Those works considered a broader range of spectral classes, not just the B0–B2 stars as we do in this work. The conclusion was reached that, despite some notable exceptions, there is little evidence that the X-ray emission from the Bp stars is different from the X-ray emission from other B stars with similar spectral types. Czesla & Schmitt (2007) carried out *Chandra* high-angular resolution observations of a sample of late B-type and A-type stars with measured magnetic fields in the range from 0.2–17 kG. They showed that the existence of a magnetic field of kG strength on a late B-type or A-type star is not necessarily a pre-requisite for finding X-ray emission among these stars.

The main focus of this work is on β Cephei-type variables and a slowly pulsating B-type star, where magnetic fields have been detected only recently. We performed dedicated observations with *XMM–Newton* for three magnetic B stars: ξ^1 CMa, V2052 Oph and ζ Cas. Two of them, V2052 Oph and ζ Cas, are detected in X-rays for the first time. We also searched the X-ray archives to collect X-ray data for other magnetic early B-type stars. Thus, at the time of writing, we have assembled a complete sample of early-type magnetic B stars for which X-ray observations are available. This sample will, undoubtedly, grow in future.

To infer stellar and wind parameters for the five stars in our sample, we employ the non-local thermodynamic equilibrium (non-LTE) stellar atmosphere model Potsdam Wolf–Rayet (PoWR) (e.g. Hamann & Gräfener 2003).

Our sample of B stars with directly measured magnetic fields is biased to non-supergiant stars. Our programme stars allow us to explore the parameter space comprising different wind momenta, field strengths and rotation periods with regard to the observed X-ray emission. We compare the properties of X-ray emission between our programme stars and other B-type stars of similar spectral types, but without a confirmed magnetic field. This allows investigation of whether the X-ray emission can serve as an indicator of the surface stellar magnetic field.

In the absence of a magnetic field, the mechanism that produces X-ray emission in early-type stars is thought to be the line-driven instability (LDI) that is an intrinsic property of stellar winds (Lucy & Solomon 1970). The LDI mechanism generates numerous shocks in a stellar wind, where plasma can be heated up to X-ray emitting temperatures (e.g. Feldmeier et al. 1997a; Feldmeier, Puls & Pauldrach 1997b).

In addition to the LDI mechanism, X-rays are thought to arise when magnetic fields are capable of governing the wind streams. Knowledge of the wind parameters, magnetic field topology and strength, together with X-ray observations, provides a good basis to review critically the models of X-ray generation in massive magnetic stars.

Groote & Hunger (1982) proposed a scenario to explain observational phenomena associated with the B2V star σ Ori E. Their model predicts the formation of a torus of matter around the star, formed by a weak stellar wind channelled along magnetic field lines. The torus is magnetically coupled to the star. Its corotation explains the observed photometric and spectroscopic variability. The X-ray emission is produced when the wind streams from opposing magnetic hemispheres collide leading to strong shock heating of the plasma. Townsend, Owocki & Ud-Doula (2007) further developed the Groote & Hunger (1982) scenario by using semi-analytical models of the rigidly rotating magnetosphere (RRM) in the limit of very strong ($\sim$few kG) magnetic fields. Their model predicts very hard X-ray emission with temperatures up to 100 MK.

Babel & Montmerle (1997b) envisage a non-rotating star with a dipole magnetic field that is sufficiently strong to confine the stellar wind. Collision between the wind components from the two hemispheres in the closed magnetosphere leads to a strong shock. The X-ray emission from the Ap-type star IQ Aur was explained in the framework of this 'magnetically confined wind shock model' (MCWS), and the presence of a magnetic field in the O-type star θ^1 Ori C was postulated (Babel & Montmerle 1997a). The direct confirmation of the magnetic field in this star by Donati et al. (2002) proved that X-rays have diagnostic potential in selecting massive stars with surface magnetic fields. Numerical magnetohydrodynamics (MHD) simulations in the framework of the MCWS model were performed by ud-Doula & Owocki (2002). These simulations compare well with the X-ray observations of θ^1 Ori C (Gagné et al. 2005); however, the model has difficulties in describing the X-ray emission from other magnetic O-type stars (Nazé et al. 2010). In this paper we discuss the applicability of the MCWS model to the early-type magnetic B stars.

Cassinelli et al. (2002), Maheswaran (2003), Brown, Cassinelli & Maheswaran (2008) and Maheswaran & Cassinelli (2009) studied the case of fast rotating magnetic massive stars with an increasing degree of model sophistication to address the formation of discs in classical Be-type stars. They showed that magnetic torquing and channelling of wind flow from intermediate latitudes on a B star could, for plausible field strengths, create a dense disc a few stellar radii in extent in which the velocity is azimuthal and of the order of the local Keplerian speed. Unlike all the other magnetically guided wind scenarios mentioned, the disc model proposed by Brown et al. (2008) is in a steady state, wind inflow being offset by a very slow outflow across reconnecting field lines. Li et al. (2008) proposed a model, where the X-rays are produced by wind material that enters the shocks above and below the disc region. The model by Li et al. (2008) predicts a relation between the X-ray luminosity normalized to the stellar bolometric luminosity (L_X/L_{bol}) and the

magnetic field strength in Be-type stars. Compared to the Be-type stars, the stars in our sample are slower rotators and have a lower wind density.

The paper is organized as follows. Our programme stars are introduced in Section 2. The new *XMM–Newton* observations are described in Section 3, and analyses of the X-ray spectra presented in Section 4. The X-ray properties of early-type Bp stars are discussed in Section 5. An analysis of UV spectra for our programme stars is presented in Section 6. We discuss our results in Section 7 and present a summary of the main points in Section 8.

2 THE PROGRAMME STARS

Our sample of early-type magnetic B stars with recently discovered magnetic fields includes the B0-type star τ Sco, the β Cephei-type variables β Cep, ξ^1 CMa and V2052 Oph, and the slow-pulsating B-type star (SPB) ζ Cas (see Table 1).

τ Sco is a well-studied object, which has been observed in X-rays by all the major X-ray missions. A complex magnetic field topology was discovered in τ Sco by Donati et al. (2006). τ Sco is a source of hard X-ray emission and displays narrow emission line profiles, suggesting a nearly stationary plasma (Mewe et al. 2003). Recently, τ Sco was monitored throughout its rotational cycle by the *Suzaku* X-ray observatory. Contrary to expectations, rotational modulations of X-ray emission were not detected (Ignace et al. 2010). Magnetic fields were detected on two other stars, HD 66665 and HD 63425, that are spectroscopically similar to τ Sco (Petit et al. 2011). Although it remains to compare their X-ray characteristics to τ Sco, the new discoveries suggest that τ Sco may be a prototype for a wider class of stars.

β Cep, ξ^1 CMa and V2052 Oph are β Cephei-type variables. β Cep-type stars have masses between 7 and 16 $M_\odot$ and are on the main sequence or in an early post-MS evolutionary phase (corresponding to spectral type O9–B3). Stars of this type display photometric and spectral variations caused by pulsations in low-order pressure and gravity modes of a short period (3–8 h) (Dziembowski & Pamiatnykh 1993).

A magnetic field in β Cep was detected by Henrichs et al. (2000). Based on the analysis of the *ROSAT* measurements, Donati et al. (2001) suggested that the X-rays from β Cep can be explained within the framework of the MCWS model. This model predicts rotationally modulated, strong and hard X-ray emission originating at a few stellar radii from the surface close to the disc around the magnetic equator. However, data appear not to support these predictions. X-ray multiphase high spectral resolution observations of β Cep by *XMM–Newton* and *Chandra* fail to show either rotational modulations or modulations on the time-scale of the stellar pulsations (Favata et al. 2009). The X-rays do not originate further out in the wind than 2–3 R_*, and the emission is quite soft with the bulk of X-ray emitting plasma at $T \approx 3$ MK, (Favata et al. 2009). The X-ray luminosity of β Cep is not atypical of stars with the same spectral type.

Hubrig et al. (2006) and Silvester et al. (2009) measured magnetic fields in a sample of eight β Cep-type stars. Both these studies agree on the lack of a definite detection of magnetic fields in the six β Cep-type stars, with typical longitudinal field formal errors of a few tens of G. The results of these investigations seem to indicate that the presence of a strong magnetic field is not a general intrinsic property of this spectral class.

Magnetic field measurements of ξ^1 CMa were reported in Hubrig et al. (2006) and confirmed by Silvester et al. (2009). Recently, Hubrig et al. (2011) established the magnetic field configuration, and the rotational periods for a number of magnetic B stars, among them is ξ^1 CMa. It was shown that we see ξ^1 CMa nearly rotational pole-on.

ξ^1 CMa was previously observed in X-rays by *Einstein* and *ROSAT*. Cassinelli et al. (1994) presented a *ROSAT* Position Sensitive Proportional Counter (PSPC) spectrum of this star. They reported a temperature of 3.7 MK and an emission measure EM $\sim 10^{54}$ cm^{-3}, and pointed out that ξ^1 CMa has the highest X-ray

Table 1. Magnetic early B-type stars with available X-ray observations.

Name	HD	Sp	B^a (G)	$v \sin i$ (km s^{-1})	$P_{\rm rot}$ (d)	Dipole	Obliquity^b β	Ref.
τ Sco	149438	B0V	$\langle \sim 500 \rangle$	5	41.033	no		1
			β Cep-type and SPB-type stars					
ξ^1 CMa	46328	B0.7IV	5300 ± 1100	9 ± 2	2.18	yes	79°	2
β Cep	205021	B2III	360 ± 40	27 ± 2	12.000 89	yes	$85° \pm 10°$	3, 4
V2052 Oph	163472	B1V	250 ± 190	60 ± 4	3.638 83	yes	$35° \pm 18°$	5
ζ Cas	3360	B2IV	335^{+120}_{-65}	17 ± 3	5.370 45	yes	$77° \pm 6°$	6
			Peculiar B stars					
y NU Ori	37061	B0V(n)	~620	225 ± 50		yes		7
V1046 Ori	37017	B2V	$\langle \sim 1500 \rangle$	$\lesssim 95$	0.9	?	42°–59°	8, 9, 13
HR 3089	64740	B1.5Vp	$\langle 572 \pm 114 \rangle$	160	1.33	?		9, 13, 14
LP Ori	36982	B2Vp	~1100	80 ± 20		yes		7
σ Ori E	37479	B2Vp	~10 000	140 ± 10	1.191	yes	66°	10
HR 5907	142184	B2.5Ve	~20 000	280	0.5083	yes (?)	4° (?)	11, 12

[a] For dipole field configuration, B is the polar field strength. For τ Sco, HR 3089 and V1046 Ori, an approximate average field strength is shown in angular brackets.

[b] β is the angle between the magnetic and rotational axes for the dipole field configuration.

References: 1, Donati et al. (2006); Sota et al. (2011); 2, Hubrig et al. (2011); 3, Telting, Aerts & Mathias (1997); 4, Donati et al. (2001); 5, Neiner et al. (2003b) 6, Neiner et al. (2003a); 7, Petit et al. (2008); 8, Bohlender et al. (1987); 9, Romanyuk & Kudryavtsev (2008); 10, Reiners et al. (2000); 11, Abt, Levato & Grosso (2002); 12, Grunhut et al. (2010); 13, Bychkov et al. (2003); 14, Borra & Landstreet (1979).

luminosity and the hardest spectrum among the β Cep-type stars in their sample.

The detection of a magnetic field in V2052 Oph was reported by Neiner et al. (2003b). The polar magnetic field was determined assuming that the star is an oblique rotator. Neiner et al. (2003b) noted that V2052 Oph is very similar to β Cep. They suggested that based on β Cep, the wind of V2052 Oph should be confined and form a disc-like structure. Prior to our observations, there was no positive detection of X-ray emission from V2052 Oph, with the *ROSAT All Sky Survey* (RASS) yielding only an upper limit to its X-ray luminosity.

The slow-pulsating B stars are slightly less luminous and cooler than the β Cep-type stars. These stars show multiperiodic brightness and colour variations on a time-scale of 0.8–3 d. Neiner et al. (2003a) reported the discovery of a magnetic field on the SPB star ζ Cas. Hubrig et al. (2006) and Silvester et al. (2009) searched for magnetic fields in a large sample of SPB stars; however, the results of their measurements agree only partially – both studies detect a magnetic field on 16 Peg (B3V) [Silvester et al. (2009) report a marginal detection]. 16 Peg is not yet detected in X-rays. Prior to our observations, there were no positive detection of X-ray emission from ζ Cas either, with the RASS yielding an upper limit to its X-ray luminosity. Neiner et al. (2003a) analysed the magnetic field configuration of ζ Cas and concluded that the star is an oblique magnetic dipole. However, they argued that there is no evidence for a disc around this star, based on the lack of an infrared (IR) excess.

3 OBSERVATIONS

We obtained dedicated *XMM–Newton* observations of ξ^1 CMa, ζ Cas and V2052 Oph. All three (MOS1, MOS2 and PN) detectors on the European Photon Imaging Camera (EPIC) were operated in the standard, full-frame mode and a thick UV filter (Strüder et al. 2001; Turner et al. 2001). The log of observations is shown in Table 2. The data were analysed using the software SAS 9.0.0. Each of the stars in our sample was detected by the standard source detection software. The exposure times and EPIC PN count rates for our programme stars are given in Table 2. The spectra and light curves were extracted using standard procedures. The spectra of all sources were extracted from regions with diameter $\approx$15 arcsec. The background areas were chosen in nearby areas free of X-ray sources. The EPIC PN spectra of ξ^1 CMa were corrected for 'out-of-time events'.

4 X-RAY SPECTRA AND THEIR FITTING

To analyse the spectra we used the standard spectral fitting software XSPEC (Arnaud 1996). The reference abundances were set to solar values according to Asplund et al. (2009). The number of counts per bin in the spectra of ζ Cas and V2052 Oph is small, therefore we used Cash statistic (Cash 1979) to fit their spectra, while the ξ^1 CMa spectra were fitted using the χ^2 statistics. Using the neutral hydrogen column density as a fitting parameter does not yield a sensible constraint on its value. Therefore, $N_{\rm H}$ was fixed at its interstellar value as found from the analysis of optical and UV spectra (see Section 6) for all our programme stars.

Table 2. *XMM–Newton* observations of three magnetic early B-type stars.

Star	MJD	Useful exposure (ks)	PN count rate[a] (s^{-1})
ξ^1 CMa	55046.4576	6.9	0.61 ± 0.01
V2052 Oph	55077.0906	9.2	0.003 ± 0.001
ζ Cas	55046.4576	12.3	0.040 ± 0.002

[a] In the 0.3–7.0 keV band; background subtracted.

The standard model *vapec*, which assumes that the plasma is in collisional ionization equilibrium (CIE), was used to model the observed X-ray spectra of our programme stars. CIE models require that several equilibria exist in the stellar wind namely that the electrons and ions are both thermalized and have equilibrated so as to have $T_{\rm e} = T_{\rm i}$ and that ionization and recombination rates are balanced. The thermalization processes is controlled by Coulomb collisions or even faster plasma effects. However, cooling of the plasma can be faster than the overall recombination time due to some ions with important cooling lines. Sutherland & Dopita (1993) provide a comparison of the collisional equilibrium time-scale and the cooling time-scale for carbon and iron ions. From their fig. 15, at temperatures above $\gtrsim$1 MK, the cooling time is $\tau_{\rm cool} = 1.5nkT/n_{\rm e}n_{\rm i}\Lambda(T) > 5 \times 10^8/n_{\rm e})$ h, and the collisional equilibrium time for C VI is $\tau_{\rm recomb} = \alpha^{-1}_{\rm recomb} \times n_{\rm e}^{-1} < 1.5 \times 10^8 (1\,{\rm cm}^{-3}/n_{\rm e})$ h, where $n_{\rm e}$ and $n_{\rm i}$ are electron and ion number densities, respectively, in cm^{-3}; $\Lambda(T)$ is the cooling function; and $\alpha_{\rm recomb}$ is the recombination coefficient [see Sutherland & Dopita (1993) for details]. Hence, at the temperatures where the maximum of emission measure is determined from the analysis of X-ray spectra (see Table 3), the cooling of the plasma is slower than the recombination time-scale, and the conditions for establishing the CIE seem to be fulfilled.

Using ξ^1 CMa as an example, we deduce from our wind models (see Section 6) that at 1 R_* distance from the photosphere, the electron density in the wind is $\sim 10^7$ cm^{-3}. The cooling time of a 1-MK plasma is $\approx$50 h while the collisional equilibrium time for C VI is $\approx$15 h. Note that this is long compared to the pulsational time-scale of β Cep-type variables, e.g. the pulsational period of ξ^1 CMa is 5.03 h (Stankov & Handler 2005).

The mean free path for a Coulomb collision $l_{\rm mfp} \approx 9.4 \times 10^7 T^2 n_8^{-1}$ cm, where T is in the units of MK, and n_8 is in the units of 10^8 cm^{-3}. Using parameters for ξ^1 CMa close to the stellar surface, the value of $l_{\rm mfp}$ is only 100 cm. Therefore, we believe that the use of CIE models to describe the X-ray spectra of our programme stars is justified.

The chemical abundances of our programme stars deviate from the solar, which is most likely a consequence of the surface magnetic field. Peculiar abundances are often found in magnetic stars, and is commonly explained by diffusion processes which allow heavier elements to sink in the atmosphere under the influence of gravity, while lighter elements are lifted to the surface by radiation pressure. The summary of the relevant publications with analyses of abundances in our programme stars can be found in Neiner et al. (2003a, 2003b) and Morel, Hubrig & Briquet (2008). In summary, these studies agree that the magnetic stars show an overabundance of nitrogen, and sometimes of helium. The quality of the X-ray spectra is not sufficient to constrain abundances. Therefore, for each star we have used the abundances determined by Morel et al. (2008).

ξ^1 CMa. The observed EPIC spectra of ξ^1 CMa and the fitted model are shown in Fig. 1. The abundances were set to solar values, except $C/C_\odot = 0.56$, $N/N_\odot = 1.48$ and $O/O_\odot = 0.79$, as found by Morel et al. (2008). We initially attempted to fit the spectra using two-temperature models similar to Favata et al. (2009) for modelling the β Cep X-ray spectrum. However, we found that adding a softer model component with kT $\approx$ 0.1 keV significantly improved the quality of the fit. Parameters of the best-fitting model are shown in Table 3. We also attempted to fit the ξ^1 CMa spectrum assuming a higher temperature component. By analogy with the τ Sco spectral

Table 3. The spectral parameters derived from the *XMM–Newton* EPIC observations of our programme stars assuming the multitemperature CIE plasma models (*vapec*) corrected for the interstellar absorption (*tbabs*). The values that have no error have been frozen during the fitting process. The corresponding spectral fits are shown in Figs 1, 3 and 2. For comparison, the spectral parameters inferred from modelling *XMM–Newton* data of β Cep and *Suzaku* spectra of τ Sco are also shown.

Star	ξ^1 CMa	ζ Cas	V2052 Oph	β Cep[a]	τ Sco[b]
$N_{\rm H}^{c}$ (10^{20} cm^{-2})	1.4	3	15	2.5 ± 0.1	3
kT_1 (keV)	0.12 ± 0.01	0.08 ± 0.02	0.14 ± 0.12	0.24 ± 0.01	0.11 ± 0.01
EM$_1$ (10^{53}cm^{-6})	22.48 ± 5.64	1.29 ± 1.05	0.006 ± 0.025	11 ± 2	17.0 ± 2.61
kT_2 (keV)	0.32 ± 0.01	0.31 ± 0.02			0.34 ± 0.01
EM$_2$ (10^{53}cm^{-3})	19.3 ± 3.36	0.27 ± 0.07			10.4 ± 0.51
kT_3 (keV)	0.68 ± 0.05		0.65 ± 0.11	0.69 ± 0.03	0.71 ± 0.10
EM$_3$ (10^{53} cm^{-6})	6.41 ± 2.57		0.003 ± 0.002	1.3 ± 0.3	7.2 ± 0.3
kT_4 (keV)					1.52 ± 0.06
EM$_4$ (10^{53} cm^{-6})					5.2 ± 0.3
$\langle kT \rangle \equiv \sum_i kT_i \times {\rm EM}_i / \sum_i {\rm EM}_i$ (keV)	0.3	0.1	0.3	0.3	0.5
Flux[d] (10^{-12} erg cm^{-2} s^{-1})	1.1	0.093	0.006	1.0	16.4

[a] The values are adopted from Favata et al. (2009).
[b] The values are adopted from Ignace et al. (2010).
[c] Correspond to the ISM hydrogen column density for all stars.
[d] In the 0.3–7.0 keV band, except of τ Sco in the 0.3–10.0 keV band, absorbed.

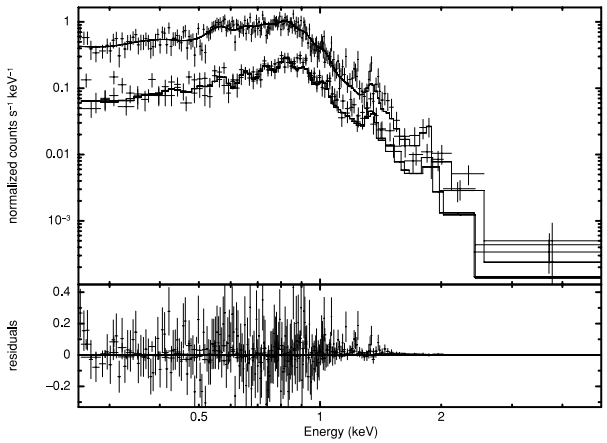

Figure 1. *XMM–Newton* PN (upper curve), and MOS1 and MOS2 (lower curves) spectra of ξ^1 CMa with the best-fitting three-temperature model (solid lines). The model parameters are shown in Table 3.

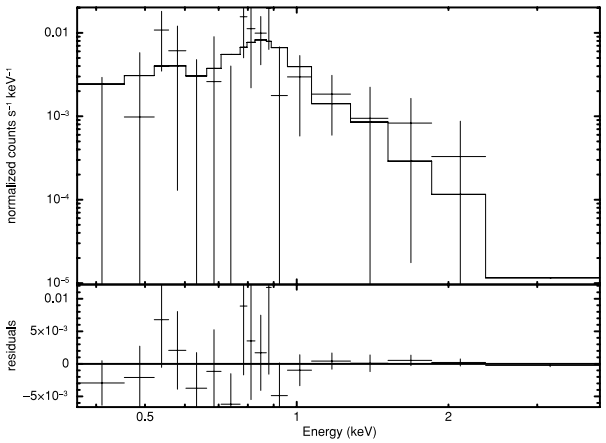

Figure 2. *XMM–Newton* EPIC-PN spectrum of V2052 Oph and the best-fitting two-temperature model. The model parameters are shown in Table 3.

models (Mewe et al. 2003), a spectral model component with $kT_4 = 1.7$ keV was assumed. However, the emission measure of this hot component cannot be constrained. As a next step, we investigated whether the ξ^1 CMa spectrum can be fitted with non-equilibrium ionization models. Using the *nei* model available in XSPEC, we failed to find a suitable set of model parameters to reproduce the observed spectrum.

V2052 Oph. Our *XMM–Newton* observation detected the X-ray emission from V2052 Oph for the first time. The source has a very low count rate (see Table 2); in total only about 60 source counts were collected. At a distance of $d = 417$ pc, the X-ray luminosity of V2052 Oph is only $L_{\rm X} \approx 3 \times 10^{29}$ erg s^{-1}, making it one of the least X-ray luminous early-type B stars in the sky. To model the observed low signal-to-noise ratio (S/N) spectrum, we fixed the neutral hydrogen column density at its interstellar value. The PN spectrum of V2052 Oph (Fig. 2) can be well described using a two-temperature plasma model (see Table 3). The abundances C/C$_\odot = 0.6$, N/N$_\odot = 1.4$ and O/O$_\odot = 0.5$ were used as found by Morel et al. (2008). The temperature and the emission measure of soft component are only poorly constrained but the presence of a soft component is required to reproduce the observed hardness ratio. There are no indications of a harder component being present in the spectrum of V2052 Oph.

Pausing to consider the X-ray spectral analyses of the β Cep-type stars (β Cep, ξ^1 CMa and V2052 Oph), it turns out that the spectral temperatures are similar among these stars. We define the mean spectral temperature $\langle kT \rangle$ as the emission measure weighted average temperature, with

$$\langle kT \rangle \equiv \sum_i kT_i \times {\rm EM}_i / \sum_i {\rm EM}_i . \quad (1)$$

Then, the mean spectral temperature for all magnetic β Cep-type stars is the same at $\approx$3.5 MK (see Table 3). However, we find a large difference in X-ray luminosities for the β Cep stars, with ξ^1 CMa being four times more X-ray luminous than β Cep and 50 times more X-ray luminous than V2052 Oph (see Table 1).

ζ Cas. Our *XMM–Newton* observations of ζ Cas are the first X-ray observations to yield the spectrum of a magnetic SPB star.

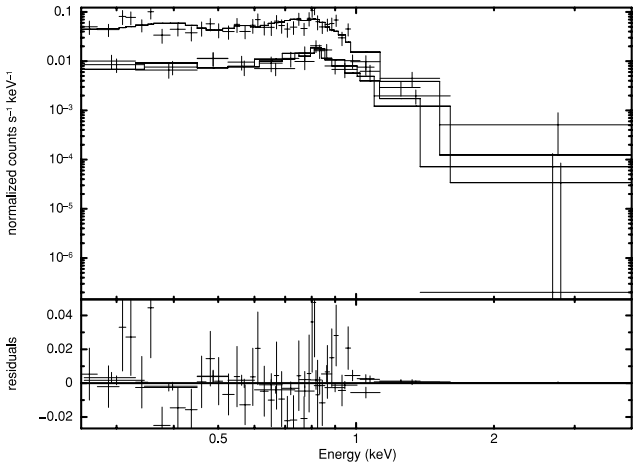

Figure 3. *XMM–Newton* EPIC PN (upper), and MOS1 and MOS2 (lower) spectra of ζ Cas and the best-fitting two-temperature model. The model parameters are shown in Table 3.

A visual inspection of EPIC *XMM–Newton* images already reveals that ζ Cas is a very soft X-ray source. This expectation is confirmed by the X-ray spectral fits. The EPIC spectra of ζ Cas and the best-fitting 2T CIE model are shown in Fig. 3. A solar composition was assumed, except for $C/C_\odot = 0.5$, $N/N_\odot = 1.4$ and $O/O_\odot = 0.5$ (Morel et al. 2008). Parameters of the model are shown in Table 3. The maximum temperature inferred from the spectral analysis is $\approx$4 MK, and there are no indications of a harder spectral component. The emission measure is dominated by the 1-MK plasma; the hotter, 4-MK component constitutes less than 20 per cent of the total emission measure. ζ Cas has the softest X-ray spectrum among all the hot stars where magnetic field have been detected. The mean X-ray spectral temperature of ζ Cas is about 1 MK (see Table 3).

5 X-RAY PROPERTIES OF CLASSICAL PECULIAR MAGNETIC EARLY-TYPE B STARS

In this section we briefly consider the X-ray properties of chemically peculiar Bp stars, addressing only stars with early spectral types. The classical chemically peculiar Bp–Ap stars have a high incidence of strong surface magnetic fields. The observed temporal variations of longitudinal magnetic fields are usually compatible with dipole or low-order multipole fields inclined to the rotation axis (Donati & Landstreet 2009). The strong magnetic fields strongly influence weak stellar winds, making the Bp stars excellent test cases for models of X-ray production in magnetic early-type stars.

There has been earlier work seeking to establish the X-ray properties of chemically peculiar stars. Drake et al. (1994) searched the RASS data base at the positions of about 100 magnetic Bp–Ap stars. They detected 10 X-ray sources and argued that in four cases the X-ray emission presumably arises from an early-type star with a radiatively driven wind. The X-ray luminosities were found to be in a general agreement with the canonical values of X-ray emission from massive stars $L_X \approx 10^{-7} L_{bol}$; e.g. the B1.5Vp star HR 3089 has $\log L_X/L_{bol} \approx -7.2$.

To include newer data, we selected Bp stars with spectral types earlier than B2 from *The Catalog of Peculiar Magnetic Stars* (Romanyuk & Kudryavtsev 2008). This sample was augmented by two more magnetic Bp-type stars reported by Petit et al. (2008) and the magnetic Be star HR 5907 recently reported by the MiMeS collaboration (Grunhut et al. 2010). As a next step we searched

Table 4. X-ray luminosities of magnetic early B-type stars.

Name	d (pc)	L_X (10^{30} erg s^{-1})	$\log (L_X/L_{bol})$
τ Sco	150	40	−6.4
Magnetic β Cep-type and SPB-type stars			
ξ^1 CMa	420	30	−6.6
β Cep	200	6.4	−7.0
V2052 Oph	400	0.3	−8.0
ζ Cas	180	0.5	−7.5
Other magnetic early-type B stars			
NU Ori	400	1.0	−8
V1046 Ori[a]	380	0.1	−8.0
HR 3089[c]	300	2	−7.2
LP Ori	470	0.02	−8.5
σ Ori E[b]	640	80	−5.6
HR 5907	120	0.4	−7.4

Distances are from van Leeuwen (2007) except of LP Ori, σ Ori E and HR 3089.
[a]The distance between the X-ray source, 2XMM J053522.0−042938 and the position of V1046 Ori is 3 arcsec.
[b]L_X (quiescent + flare) in 0.1–2.4 KeV band from Sanz-Forcada et al. (2004).
[c] L_X in 0.1–2.4 KeV band Drake et al. (1994).

the available X-ray catalogues. Our search revealed that σ Ori E, LP Ori, NU Ori and V1046 Ori, HR 5907 have positive X-ray detections.

σ Ori E is the prototypical oblique fast magnetic rotator. Its X-ray emission is quite hard: the EM of 10-MK plasma is as large as the EM of the cooler plasma with $T \approx 3$ MK (Sanz-Forcada, Franciosini & Pallavicini 2004). The mean spectral temperature of σ Ori E (in quiescence) is 0.66 keV or 7.6 MK. We estimate the bolometric luminosity of σ Ori E, $\log L_{bol}/L_\odot = 3.8$, based on its spectral type and *UBV* colours and assuming a distance of 640 pc (Hunger, Heber & Groote 1989). The average (quiescent+flare) X-ray luminosity at 640 pc is $L_X = 8 \times 10^{31}$ erg s^{-1}. Thus, the star is X-ray luminous: its ratio of X-ray to bolometric luminosities L_X/L_{bol} ratio is nearly 2 orders of magnitude higher than normally found in B-type stars (see Table 4). An extremely rare event in the history of X-ray observations of massive hot stars – an X-ray flare – has been observed from σ Ori E (Groote & Schmitt 2004; Sanz-Forcada et al. 2004) that may be understood to be a result of centrifugal breakout of the torus (Mullan 2009). These X-ray properties of σ Ori E seem to confirm the expectations of the RRM model (Townsend et al. 2007).

Given the general nature of these models, one would naturally expect that these results could be applied to other BV stars with strong magnetic fields. This, however, seems not to be the case.

The young star LP Ori is similar to σ Ori E in many respects: it has a similar age, spectral type and a kG-strong magnetic field. It is also a source of hard X-ray emission (Getman et al. 2005). However, the X-ray luminosity of LP Ori is significantly lower than the X-ray luminosity of σ Ori E. In fact, the X-ray luminosity of LP Ori is nearly the lowest one among all magnetic early B stars (see Table 4). The models predict modulations of the X-ray luminosity due to the occultation of the X-ray emitting site by the opaque torus. These modulations are thought to occur on a time-scale comparable to the rotational period of the star. LP Ori was observed by

Chandra for ≈8.8 d (Getman et al. 2005). This long exposure time suggests that the observed X-ray flux is somewhat averaged over the rotational period, and the star is indeed intrinsically faint in X-rays.

X-ray observations of σ Ori E and LP Ori seemingly suggest that the strong magnetism may account for the hardness of the X-ray emission. However, the Bp stars V1046 Ori and NU Ori provide counterexamples.

Similar to σ Ori E, V1046 Ori has a kG magnetic field. It also is an oblique magnetic rotator, whose obliquity and rotational period are similar to that of σ Ori E. The star was serendipitously observed by *XMM–Newton*. No X-ray spectra are available, but hardness ratios are provided in *The Second XMM–Newton Serendipitous Source Catalog or 2XMMi-DR3* and in Nazé (2009). We have compared these hardness ratios with those of τ Sco reported in the same catalogue. V1046 Ori is a softer X-ray source compared to τ Sco, and its X-ray luminosity is relatively low (see Table 4). We estimate its bolometric luminosity based on *UBV* colours and spectral type.

The magnetic field on NU Ori is only about ∼0.5 kG and is weaker than the fields of the other Bp stars in our sample. Petit et al. (2008, and references therein) comment on NU Ori being a triple system, containing a massive B0.5V primary, along with a low-mass spectroscopic companion and a visual companion. NU Ori was recently analysed by Simón-Díaz et al. (2011), who obtained $\log L_{\rm bol}/L_{\odot} = 4.4$. NU Ori was observed by *Chandra* simultaneously with LP Ori (Getman et al. 2005). Surprisingly, that analysis indicates that the X-ray luminosity of NU Ori is a factor of 30 higher than for LP Ori, yet the former has a considerably softer emission as compared to the latter.

HR 5907 has a very strong magnetic field (Grunhut et al. 2010). Assuming a dipole, the field strength at the pole is ≈20 kG. The star is a fast rotator with $v \sin i \approx 280\,{\rm km\,s^{-1}}$ (Abt et al. 2002). Yudin (2001) detects intrinsic polarization at the level of 0.17 per cent in *V* band and considers this star as a classical Be star with a disc. The star was observed by *ROSAT* PSPC for ≈4.8 ks. It is detected with a flux of $\approx 2 \times 10^{-13}\,{\rm erg\,cm^{-2}\,s^{-1}}$ corresponding to a rather low X-ray luminosity (see Table 4). We fit the low S/N PSPC spectra and find that HR 5907 has a relatively hard spectrum characterized by a temperature above 1 keV.

Considering just our small sample of early-type B stars with kG-strong magnetic fields, we must conclude that the new measurements confirm earlier results on the X-ray emission from Bp–Ap stars. The properties of their X-ray emission are quite diverse, with majority of the stars emitting X-rays at the level typical of the general sample of B stars (e.g. Drake et al. 1994). The rigidly rotating magnetosphere scenario makes robust predictions of strong, variable and hard X-ray emission. It appears that in five out of the six early-type magnetized B stars under discussion, these predictions are not fulfilled.

Placed in the context of this earlier work, our results corroborate the basic conclusion that while a strong and hard X-ray emission is sufficient to suggest that a star may be magnetic, it is not a required property of magnetic stars.

6 STELLAR WINDS

The strong UV radiation of B-type stars drives their stellar winds. The parameters of stellar winds are commonly inferred from the analyses of optical and UV spectral lines by means of stellar atmosphere models. While the B-type giants and supergiants have often been analysed, the winds of BIV- and BV-type stars yet remained relatively unexplored. Prinja (1989) used profile fits to model spectral lines of C IV, Si IV and Si III in high-resolution spectra of B stars obtained with the *International Ultraviolet Explorer* (*IUE*), and produced a homogeneous set of wind-velocity and column-density measurements for 40 non-emission, non-supergiant B stars. It was concluded that the presence of C IV resonance doublet in their UV spectra must be due to the effect of X-rays on wind ionization. This effect is often referred to as 'superionization'. Prinja (1989) did not find any asymmetry in the Si IV lines which would be typical if the stellar wind was strong. Estimates of column densities revealed that the mass-loss rates in non-supergiant B stars are significantly lower than in O and Be stars. From fitting the UV resonance lines of C IV and Si IV, it was found that the products of mass-loss rate and ionization fraction, $\dot{M}q$, are $\ll 10^{-10}\,{\rm M_{\odot}\,yr^{-1}}$. Regarding the wind velocities, it was shown that the winds of 'normal' non-supergiant stars are slow compared to those of the Be stars. The maximum observed wind velocities do not generally exceed the stellar escape velocity.

In this paper we analyse the UV spectra of our sample magnetic stars by means of a stellar atmosphere code. Stellar spectroscopy codes used to analyse massive stars are based on spherically symmetric or plane-parallel geometries, despite the clear observational evidence that massive star winds can deviate from spherical symmetry (e.g. Kaper et al. 1997; Hamann et al. 2001). It is very probable that magnetic fields affect the wind geometry. However, at present a 3D modelling of stellar winds that would allow quantitative spectroscopic analysis is beyond reach. Our approach allows us to conduct a quantitative multiwavelength X-ray and UV/optical spectral analysis. The obtained wind parameters allow us to compare our sample stars with other massive stars in the general framework of massive star wind quantitative spectroscopy.

6.1 Model description: PoWR stellar atmosphere

In this work we analyse the spectra of magnetic B stars by means of stellar atmosphere models that account for the presence of X-rays. We use the PoWR model atmosphere code (Hamann & Gräfener 2003, 2004). The PoWR code has been used extensively to analyse not only massive stars with strong stellar winds (e.g. Liermann et al. 2010), but also low-mass central stars of planetary nebulae, and extreme helium stars (Hamann 2010; Todt et al. 2010). The PoWR code solves the non-LTE radiative transfer in a spherically expanding atmosphere simultaneously with the statistical equilibrium equations and accounts at the same time for energy conservation. Complex model atoms with hundreds of levels and thousands of transitions are taken into account. The computations for the present paper include complex atomic models for hydrogen, helium, carbon, oxygen, nitrogen and silicon. Iron and iron-group elements with millions of lines are included in the PoWR code through the concept of superlevels (Gräfener, Koesterke & Hamann 2002). The extensive inclusion of the iron group elements is important not only because of their blanketing effect on the atmospheric structure, but also because the diagnostic wind lines in the UV (e.g. the C IV and Si IV resonance lines) are heavily blended with the 'iron forest'.

The PoWR models can take account of stellar-wind clumping in the standard volume-filling factor 'microclumping' approach (e.g. Hamann & Koesterke 1998), or even, with an approximate correction for wind clumps of arbitrary optical depth ('macroclumping', Oskinova, Hamann & Feldmeier 2007). However, since the wind signatures are quite weak for all stars of our sample, and since there is no way to estimate the degree of clumping, we apply here only smooth-wind models. Note that microclumping does not directly influence the resonance line profile shapes via radiative transfer

effects, but can indirectly affect the lines by virtue of modifying the ionization stratification.

The X-ray emission and its effects on the ionization structure of the wind is included in the PoWR atmosphere models according to the recipe of Baum et al. (1992). We assume an optically thin, hot plasma component distributed within the 'cool' stellar wind. The uniform value of the so-called emission measure 'filling factor', $X_{\rm fill} = {\rm EM_{hot}/EM_{cool}}$ (really a density squared weighted volume ratio), is adjusted such that the emergent X-ray luminosity agrees with the observations. The X-ray emissivity is restricted to the fast-wind domain, for which we assume a minimum radius of 1.1 R_*. The absorption of the X-ray radiation by the 'cool' stellar wind is taken into account, as well as its effect on the ionization stratification by the Auger process.

The lower boundary of the model atmosphere is set at a Rosseland depth of 20, meaning that the (nearly) static photosphere is included in the computations. The velocity field consists of two parts. In the photospheric part of the atmosphere, a hydrostatic density stratification is assumed, while for the wind the usual 'β-law' prescription is adopted, in our case with an exponent $\beta = 1$. We also tested the so-called double-β law (Hillier & Miller 1999), but without substantial improvement of the fit quality.

Each stellar atmosphere model is defined by the effective temperature, surface gravity, luminosity, mass-loss rate, wind terminal velocity $v_\infty$and chemical composition. The gravity determines the density structure of the stellar atmosphere below and close to the sonic point. From the pressure-broadened profiles of photospheric lines, the spectroscopic analysis allows derivation of the gravity and thus the stellar mass. For our sample of B stars, we confirm a discrepancy between the spectroscopic and evolutionary mass, the former being lower than the latter (see Weidner & Vink 2010, and references therein).

Dedicated analyses of the photospheric spectra of our programme stars have been performed by Neiner et al. (2003b), Neiner et al. (2003a) and Morel et al. (2008). Using their abundances, $T_{\rm eff}$ and $\log g$, we find that our model reproduces photospheric spectra very well, as demonstrated by the example shown in Fig. 4. Therefore, to speed up the analysis, we adopt the literature values of $T_{\rm eff}$ and $\log g$. The effects of rotation with values $v \sin i$ from Table 1 are also included in the models.

All stars in our sample have measured parallaxes. Hence we can scale synthetic spectral energy distributions (SEDs) to that distance and fit to the observations, covering the whole wavelength range from the UV to IR. Furthermore, the model spectra are corrected for interstellar extinction. Dust extinction is taken into account using the reddening law of Cardelli, Clayton & Mathis (1989). An example of SED fit is shown in Fig. 5. The figure also shows the model continuum without lines, illustrating how the 'forest' of iron lines forms a pseudo-continuum in the UV that is well reproduced by our model.

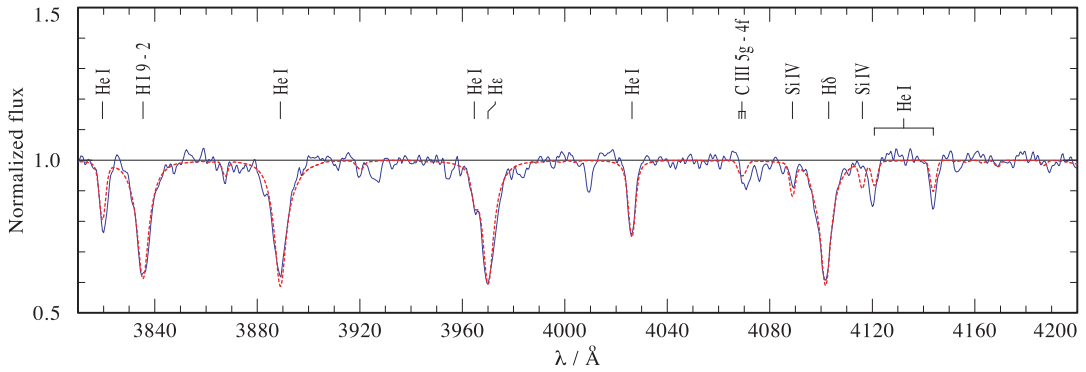

Figure 4. Optical CTIO spectrum of ξ^1 CMa obtained on 1988 November 02 (Walborn & Fitzpatrick 1990) (blue line) versus a PoWR model spectrum (red line) using the stellar parameters of ξ^1 CMa as shown in Table 6. The model spectrum is convolved with a 2.5-Å Gaussian to match the spectral resolution of the '2D-Frutti' spectrograph at CTIO.

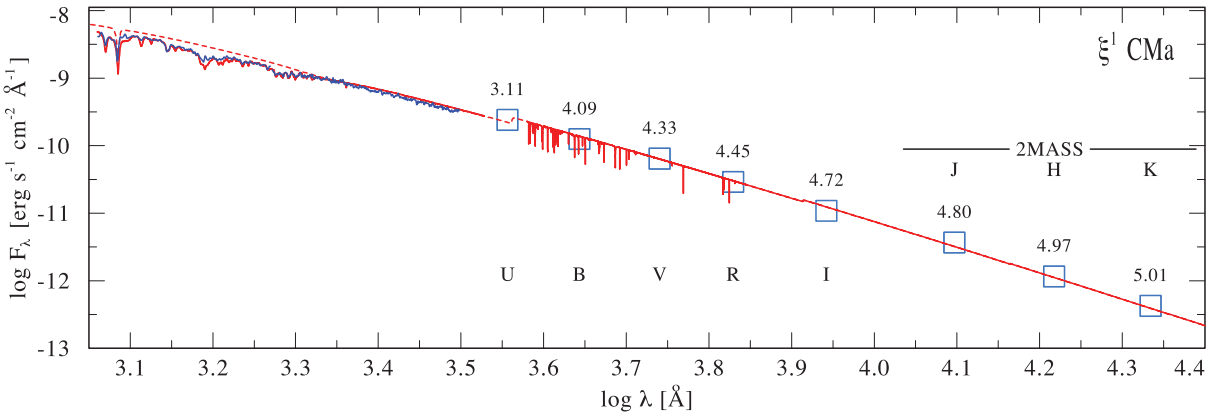

Figure 5. Spectral energy distribution for ξ^1 CMa. The observed *IUE* spectra are shown as thin blue lines. Blue boxes indicate observed photometry (labels: magnitudes) taken from the 2MASS catalogue (Skrutskie et al. 2006) and from Morel & Magnenat (1978). The synthetic spectrum (red line) is calculated using parameters given in Table 6. The model flux is reddened with $E(B-V) = 0.04$ and corrected for interstellar Lyman line absorption. The model continuum without lines (red dotted) is also shown to demonstrate how the iron group lines form a pseudo-continuum in the UV.

Table 5. UV observations of programme stars used in the analysis.

Object	Data set	Date
ζ Cas	SWP 51309	04/07/1994
ξ^1 CMa	SWP 03574	12/12/1978
τ Sco	SWP 55997	23/09/1995
V 2052 Oph	SWP 50431	31/03/1994
β Cep	SWP40477	28/12/1990

With $\log g$, $T_{\rm eff}$ and $L_{\rm bol}$ being fixed, we compare the synthetic and observed lines, varying the wind parameters $\dot{M}$ and v_∞ so as to achieve the best fit. The usual indicators of mass-loss used in B supergiants and Be stars, as well as in O-type stars, are Hα together with the UV resonance lines. However, in our sample of non-supergiant stars the Hα line is entirely photospheric.[1] Therefore, our wind diagnostic can only be based on the UV resonance lines. High-resolution *IUE* spectra were retrieved from the archive for all the stars of our sample. For some of them, multiple *IUE* observations are available (see e.g. the *IUE* time series for β Cep and ξ^1 CMa in Schnerr et al. 2008). In those cases we selected the observation of best quality (cf. Table 5).

6.2 τ Sco

τ Sco is a well-studied object that has remained one of the primary targets in stellar UV and X-ray astronomy from their early days (e.g. Rogerson & Upson 1977; Macfarlane & Cassinelli 1989). It was one of the first stars whose UV spectrum was analysed by means of atmosphere models based on comoving radiative transfer techniques by Hamann (1981), who obtained a mass-loss rate $\log \dot{M} = -8.9 \pm 0.5$ from the analysis of UV lines. It was also shown that O VI and N V lines cannot be reproduced by the cool wind models. Cassinelli & Olson (1979) explained the presence of O VI and N V as arising from Auger ionization by X-rays.

We re-analysed the wind properties of τ Sco using the PoWR model. The abundances as presented in Hubrig et al. (2008) were adopted. We obtained wind parameters by modelling the C IV, N V and Si IV lines. During our analysis we found that the line profiles in the *IUE* range are strongly influenced by a combination of three parameters at the same time: the terminal wind velocity v_∞, the mass-loss rate $\dot{M}$ and the impact of superionization via X-ray emission. It is not possible to disentangle these effects and therefore our solution may not be unique.

We include the X-ray flux and temperature as deduced from the observations. The need to account for X-rays in wind modelling can be nicely demonstrated using C IV and N V doublets (Figs 6 and 7). Although it is possible to reproduce the observed C IV doublet without X-ray superionization by assuming a lower $\dot{M}$ and a lower v_∞, this method fails for the N V doublet. As the effective temperature of B stars is not high enough to create sufficient amounts of N V by photoionization, the observed P Cygni line profile of the N V doublet can only be reproduced if superionization due to X-rays is included. On the other hand, the Si IV doublet in τ Sco has little sensitivity to the X-rays (Fig. 8).

With fixed parameters for the X-ray emitting gas from this study, the terminal velocity of the wind can be deduced from fitting the line profiles. Fig. 9 shows the asymmetric line profile of the C IV-line doublet at $\lambda\lambda$ 1548.2, 1550.8 Å. We calculated three models taking $v_\infty = 500$, 1000 and 1500 km s^{-1} and keeping other parameters the same. Although a higher wind velocity cannot be excluded, we find that a model with $v_\infty = 1000$ km s^{-1} described the observed lines best.

Setting $v_\infty = 1000$ km s^{-1}, attention was next directed towards the determination of the mass-loss rate. Models with mass-loss rates in the range of $\log(\dot{M}/{\rm M}_\odot\,{\rm yr}^{-1}) = -9.3, \ldots, -8.6$ were computed and compared to the UV data. We were not able to find a unique solution which could describe all lines equally well. The C IV doublet is better reproduced with a lower $\dot{M} = 10^{-9.3}\,{\rm M}_\odot\,{\rm yr}^{-1}$ as illustrated in Fig. 10. This mass-loss rate is also favoured by the model fitting of the N V doublet (see Fig. 11). On the other hand, Si IV doublet is best described by a model with a higher mass-loss of $\dot{M} = 10^{-8.6}\,{\rm M}_\odot\,{\rm yr}^{-1}$ as shown in Fig. 12.

The steps as described above were performed for all our programme stars.

6.3 β Cep

β Cep is a well-studied object. Despite this, to our knowledge, there has been no prior detailed modelling of the UV resonance lines

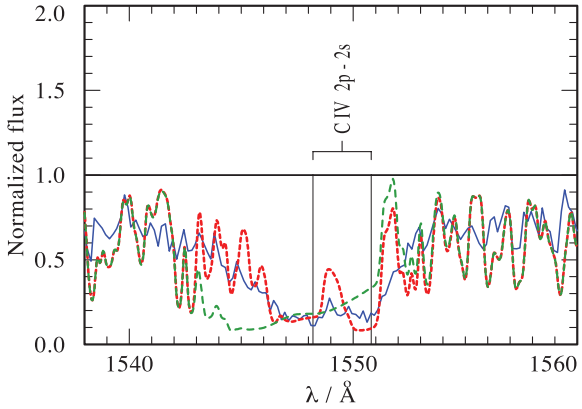

Figure 6. τ Sco: the effect of ionization by X-rays on C IV $\lambda\lambda$1548.2, 1550.8 Å doublet. Details of the UV spectrum observed with *IUE* (blue thin line) versus PoWR models: without X-rays (green dotted line) and with X-rays (red thick line). Model parameters: $\log(\dot{M}) = -9.3$, $v_\infty = 1000$ km s^{-1}. This figure shows that C IV is efficiently destroyed by X-rays in the outer parts of the atmosphere. Without accounting for the ionization by X-rays, the mass-loss rate would be underestimated.

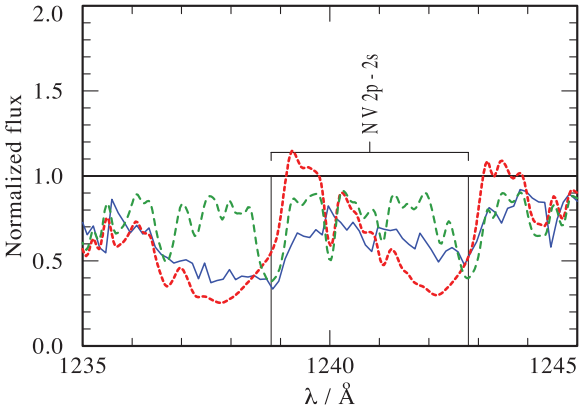

Figure 7. τ Sco: same as in Fig. 6 but centred on the N V doublet.

[1] β Cep shows Hα emission episodes. However, Schnerr et al. (2006) found that the Hα emission is not related to the primary in β Cep, but is due to its 3.4-mag fainter companion that is a classical Be star.

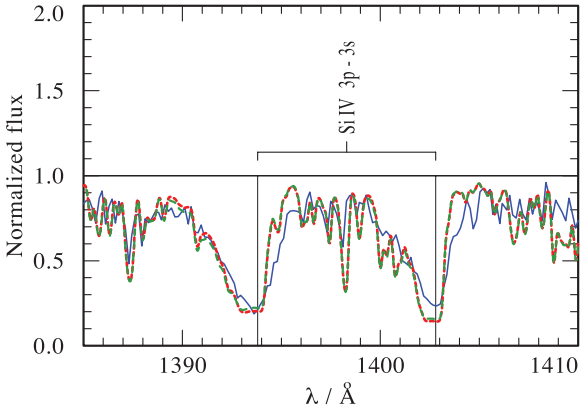

Figure 8. τ Sco: same as in Figs 6 and 7 but centred on the Si IV doublet. Model parameters: $\log(\dot{M}) = -8.6$, $v_\infty = 1000\,\mathrm{km\,s^{-1}}$. Note that even without X-rays, most silicon is already ionized to Si V in the outer parts of the atmosphere, therefore the Si IV doublet is insensitive to X-rays.

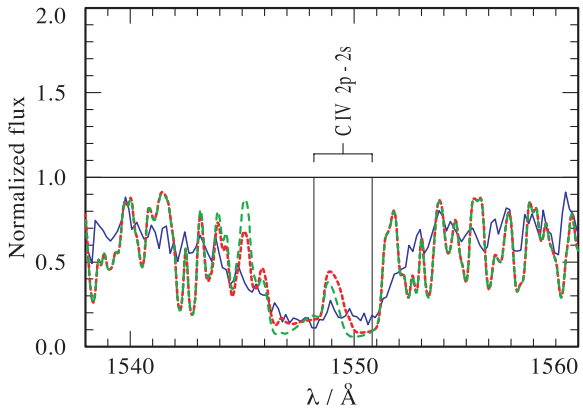

Figure 9. τ Sco: determination of the wind velocity from modelling the C IV line. Details of the UV spectrum observed with *IUE* (blue thin line) versus PoWR models with $v_\infty = 500\,\mathrm{km\,s^{-1}}$ (green dotted line) and $v_\infty = 1000\,\mathrm{km\,s^{-1}}$ (red dotted line). The derived mass-loss rate is $\log(\dot{M}) = -9.3$. The blue absorption wing of the C IV line is better matched by the model with a higher v_∞. Both models include ionization due to X-rays with parameters as listed in Table 1.

from this star. Donati et al. (2001) adopted a terminal wind velocity of $v_\infty = 900\,\mathrm{km\,s^{-1}}$. Using a constraint on the product $\dot{M}q$(C IV) obtained by Prinja (1989), and adopting an ionization fraction of C IV at 0.1 per cent, Donati et al. estimated a mass-loss rate of $\log \dot{M} = -9$ for β Cep. They also noticed that this mass-loss rate is significantly lower than the predicted value of $2.4 \times 10^{-8}\,\mathrm{M_\odot\,yr^{-1}}$ for a CAK model (Castor, Abbott & Klein 1975) of a star like β Cep (Abbott 1982).

The ionization fractions of carbon obtained by detailed modelling of the β Cep atmosphere with the PoWR code are shown in Fig. 13. The effect of ionization by X-rays prevents C IV from being the dominant ion anywhere in the stellar wind except right at the photospheric level. Therefore systematically lower mass-loss rates would be obtained from the modelling of the C IV doublet by models that do not account for the X-rays. (The effect is illustrated in Fig. 6 using τ Sco as an example.)

Schnerr et al. (2008) studied the wind-line variability in magnetic B stars. They considered all the 81 UV spectra of β Cep available in the *IUE* archive and showed that the C IV doublet is strongly modulated with the rotation period of 12 d. Their fig. 2 shows the gradual transition from an enhanced to a reduced contribution of

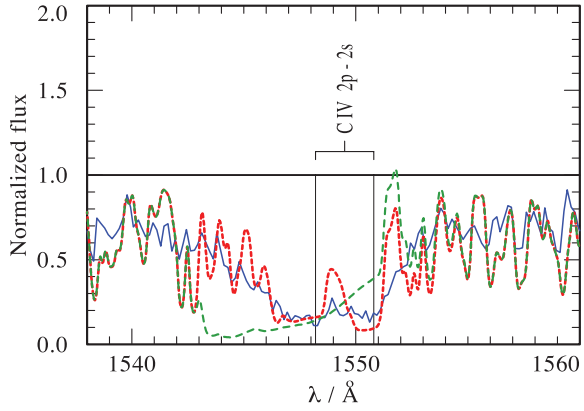

Figure 10. τ Sco: constraining the mass-loss rate from modelling of the C IV doublet. Details of the UV spectrum observed with *IUE* (blue thin line) versus PoWR models with $\log \dot{M} = -8.6$ (green dotted line) and $\log \dot{M} = -9.3$ (red dotted line). Both models use $v_\infty = 1000\,\mathrm{km\,s^{-1}}$ and include superionization. The C IV doublet is better matched by the model with the lower $\dot{M}$.

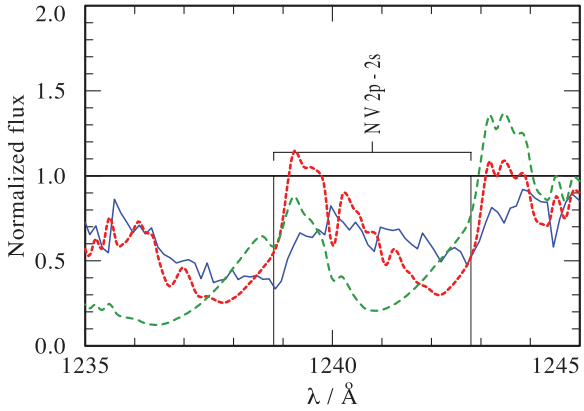

Figure 11. τ Sco: same as in Fig. 10 but for the N V doublet. The P Cygni line profile of the N V doublet is strongly affected by X-ray ionization. The observed line is better fitted by a model with a low mass-loss rate $\log \dot{M} = -9.3$ (red dotted line).

emission centred close to zero velocity in C IV, as typical in magnetic B stars.

Fig. 14 shows the observed C IV doublet compared to a model that assumes $v_\infty = 700\,\mathrm{km\,s^{-1}}$ and $\log \dot{M} = -9.4$. A higher mass-loss rate of $\log \dot{M} = -9.1$ is required to reproduce the Si IV line, as shown in Fig. 15.

6.4 ξ^1 CMa

This is the first analysis of the UV spectral lines of the β Cep-type star ξ^1 CMa by means of stellar atmosphere models.

In modelling the spectrum of this object, we note that the *IUE* data of this star are of rather low quality. It seems that the background subtraction was not performed correctly, because the minimum of the interstellar Lyman α absorption line is not 'black' as it should be. Therefore we adjusted the background level accordingly. Our model reproduces the broad SED from the UV to the IR very well (see Fig. 5). Fig. 4 shows our model compared to the optical spectrum of ξ^1 CMa – the model produces quite a good match to the line spectra. Therefore, it is surprising that we were not able to achieve good-quality fits to the C IV (see Fig. 16) and N V lines.

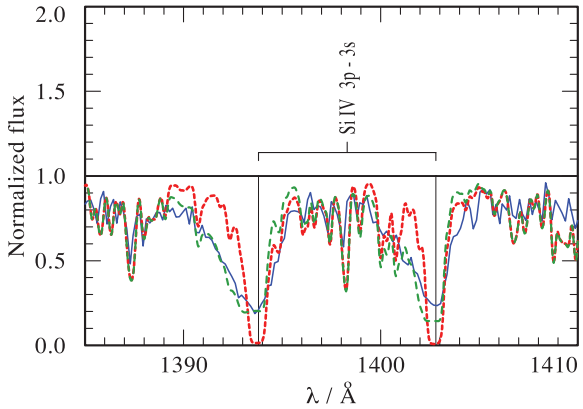

Figure 12. τ Sco: same as in Figs 10 and 11 but for the Si IV doublet. In contrast to the C IV and N V doublets, the observed doublet of Si IV is better matched by a model with a higher mass-loss of $\log \dot{M} = -8.6$.

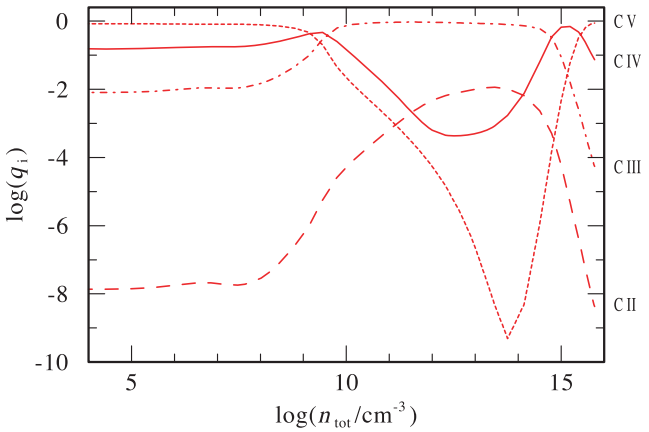

Figure 13. Relative ionization fractions of carbon in the wind of β Cep as a function of density in the wind, with declining density corresponding to larger radius. The wind model is calculated with $v_\infty = 700\,\mathrm{km\,s^{-1}}$, $\log \dot{M} = -9.4$; stellar parameters are taken from Table 6.

It is tempting to suggest that the reason for these modelling difficulties may be due to the pole-on orientation of ξ^1 CMa (Hubrig et al. 2011), although the poor quality of the data is a concern as well. The observed line profiles of Si IV (see Fig. 17) are roughly reproduced by our model. We adopted a larger turbulence in the wind compared to the photosphere and convolved the UV model spectra with a Gaussian of 1-Å full width at half-maximum (FWHM), corresponding to a turbulence velocity of about 200 km s^{-1}.

For β Cep and V2052 Oph, the mass-loss rate required to reproduce the Si IV doublet is higher as compared to what is needed to fit C IV, an effect that we attribute to the superionization by X-rays. This, however, is not the case for ξ^1 CMa. Fig. 16 shows the C IV line compared to model line with $\log \dot{M} = -10$, as obtained from the analysis of Si IV.

Schnerr et al. (2008) presented a time-series analysis of *IUE* observations of the C IV doublet in ξ^1 CMa and noticed a lack of temporal modulations in the spectra. Increasing the mass-loss rate would result in a stronger absorption feature, which is not observed. Therefore, we conclude that the UV lines in ξ^1 CMa are peculiar compared to other magnetic stars in our sample, either due to the quality of the observations or reflecting the intrinsic peculiarity to the source itself.

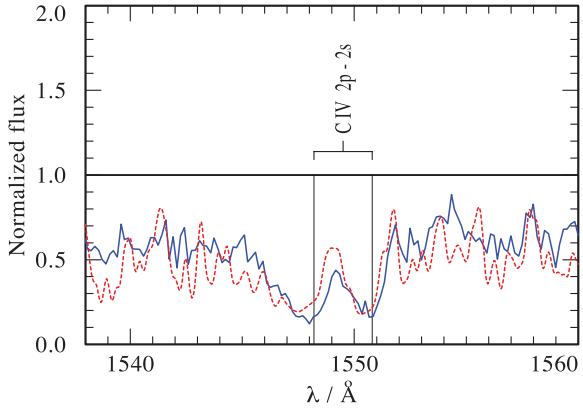

Figure 14. β Cep: details of the UV spectrum observed with *IUE* (blue thin line) versus PoWR models with $v_\infty = 700\,\mathrm{km\,s^{-1}}$ and $\log \dot{M} = -9.4$ (red dotted line). The C IV λλ1548.2, 1550.8 Å doublet is shown.

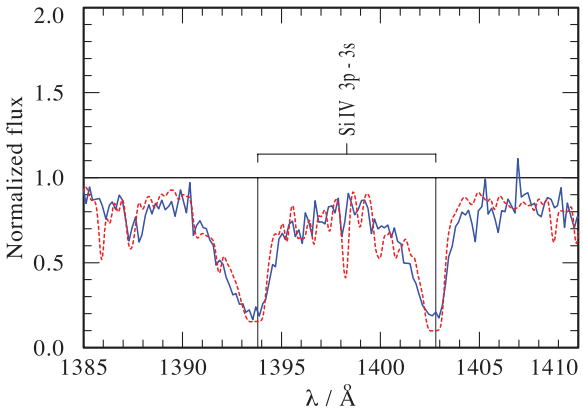

Figure 15. β Cep: the same as in Fig. 14 and but for the Si IV λλ1393.8, 1402.8 Å doublet. A PoWR model with $\log \dot{M} = -9.1$ (red dotted line) is shown.

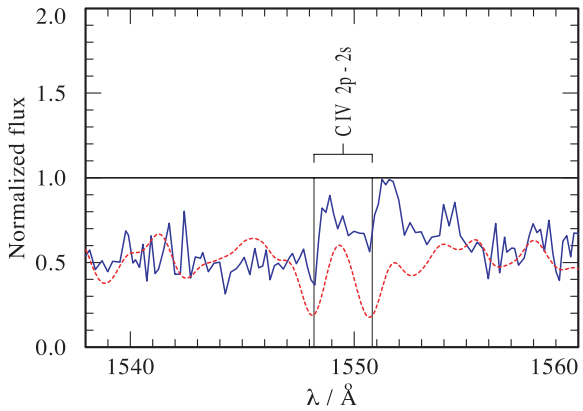

Figure 16. ξ^1 CMa: details of the UV spectrum observed with *IUE* (blue thin line) versus PoWR models with $v_\infty = 700\,\mathrm{km\,s^{-1}}$ and $\log \dot{M} = -10$ (red dotted line). The C IV λλ1393.8, 1402.8 Å doublet is shown.

6.5 V2052 Oph

This is the first analysis of wind properties of V2052 Oph. As with the previous stars (except τ Sco), we adopt a wind terminal velocity of $v_\infty = 700\,\mathrm{km\,s^{-1}}$. We did calculate models with $v_\infty = 1000\,\mathrm{km\,s^{-1}}$, but results were similar. Fig. 18 shows the C IV doublet in the *IUE* spectrum of V2052 Oph compared to a wind model

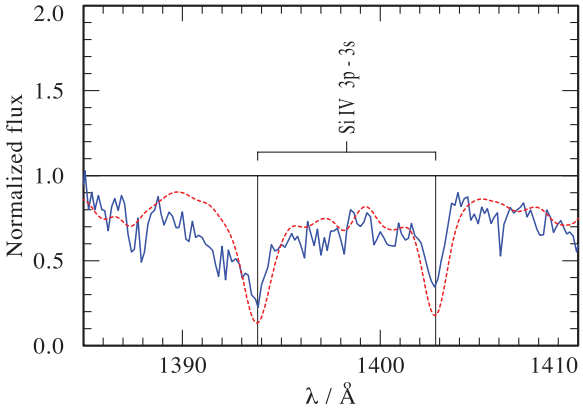

Figure 17. ξ^1 CMa: the same as in Fig. 16 but for the Si IV λλ1393.8, 1402.8 Å doublet.

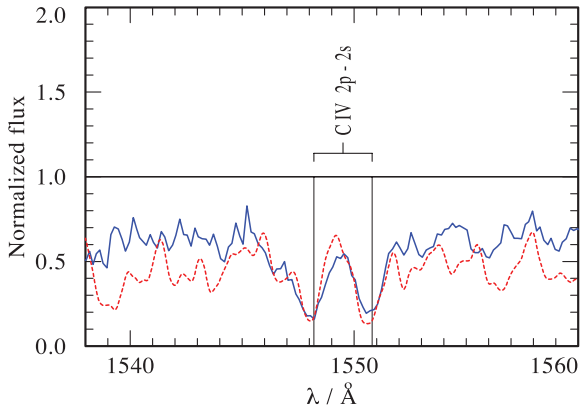

Figure 18. V2052 Oph: details of the UV spectrum observed with *IUE* (blue thin line) versus PoWR models with $v_\infty = 700\,\mathrm{km\,s^{-1}}$ and $\log \dot{M} = -10.7$ (red dotted line). The C IV λλ1548.2, 1550.8 Å doublet is shown.

with $\log \dot{M} = -10.4$. The effective temperature of V2052 Oph is relatively low at $T_{\rm eff} = 23$ kK, and C III would have been the leading ionization stage if there were no X-ray emission. As with other stars in our sample, the effect of superionization proves critical, in this case elevating the ionization fraction of C IV in the wind.

We were not able to achieve a satisfactory fit to the N V doublet with a model that includes X-ray emission. This line is very sensitive to the presence of ionizing photons in the wind, and even models with a mass-loss as low as $\log \dot{M} = -10.7$ produces an N V doublet that is stronger than observed. This is an interesting challenge because the observed level of X-ray emission in V2052 Oph is quite low, smaller than in the other stars of our sample.

Similarly to results for other programme stars, the Si IV doublet is better reproduced with models that assume higher mass-loss rates than required for the C IV and N V doublets. Fig. 19 shows a model fit with $\log \dot{M} = -9.7$ to the Si IV lines. Note that the low $T_{\rm eff}$ of about 23 kK would normally suggest that the dominant ion stage of silicon would be Si IV; however, with the presence of X-rays, Si V becomes the dominant ion, and the Si IV doublet shows a more photospheric absorption profile.

6.6 ζ Cas

Ours is the first analysis of the wind properties of ζ Cas. This star is the coolest among our sample. Again, we fixed the parameters

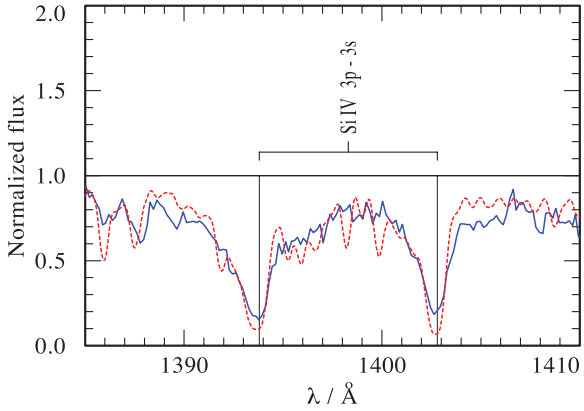

Figure 19. V2052 Oph: the same as in Fig. 18 but for the Si IV λλ1393.8, 1402.8 Å doublet. A PoWR model with $v_\infty = 700\,\mathrm{km\,s^{-1}}$ and $\log \dot{M} = -9.7$ (red dotted line) is shown.

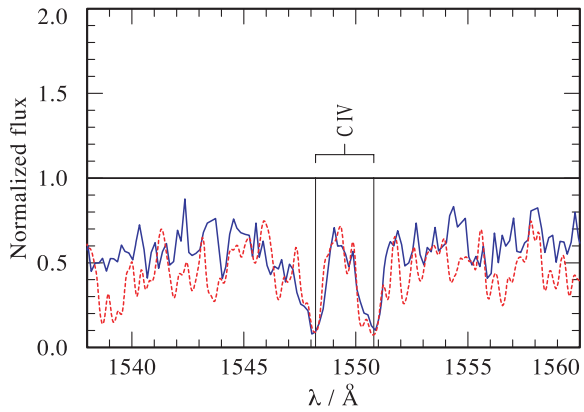

Figure 20. ζ Cas: details of the UV spectrum observed with *IUE* (blue thin line) versus PoWR models with $v_\infty = 700\,\mathrm{km\,s^{-1}}$ and $\log \dot{M} = -11$ (red dotted line). The C IV λλ1548.2, 1550.8 Å doublet shows a purely photospheric absorption profile without any wind signature.

of X-ray emission based on *XMM–Newton* data, and calculated a range of models for various values of v_∞ and $\dot{M}$.

Fig. 20 shows the observed C IV doublet plotted together with a PoWR model. The observed line shows a purely photospheric absorption profile without any wind signature and is quite well fitted with a PoWR model. From such a photospheric absorption profile, it is not possible to infer the wind velocity. We have therefore assumed a terminal wind speed of $v_\infty = 700\,\mathrm{km\,s^{-1}}$.

Wind emission signatures are present in the N V doublet as seen in Fig. 21. Note that the model N V line has a P Cygni line profile because N V becomes the leading ionization stage via the effect of superionization. However, in order to reproduce this line we have to adopt a small mass-loss rate of only $\log \dot{M} = -11$. Surprisingly, even with this mass-loss rate, the model line is somewhat stronger than observed.

Similarly to other stars, there is no unique solution for the mass-loss rate, with different UV lines indicating somewhat different mass-loss rates. Fig. 22 shows models of Si IV compared with the *IUE* data. At a low T_* of about 21 kK, Si IV would be the dominant ion stage, but X-ray emissions make Si V the dominant ion in the wind so that the Si IV line shows a more photospheric absorption profile.

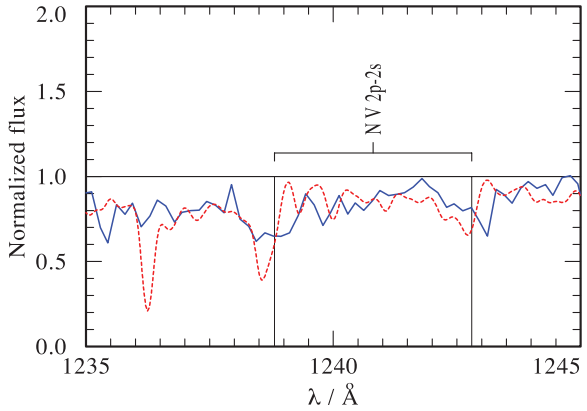

Figure 21. ζ Cas: same as in Fig. 20 but for the N v $\lambda\lambda$1238.81, 1242.8 Å doublet.

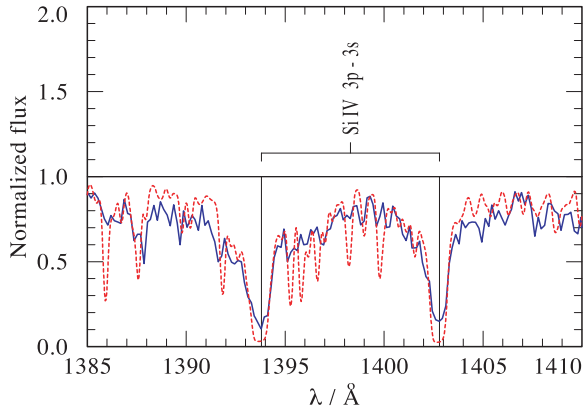

Figure 22. ζ Cas: the same as in Figs 20 and 21 but for the Si IV $\lambda\lambda$1393.8, 1402.8 Å doublet. A PoWR model with $v_\infty = 700\,\mathrm{km\,s^{-1}}$ and $\log \dot{M} = -9.7$ (red dotted line) is shown.

6.7 Uncertainties in $\dot{M}$ determination in non-supergiant B stars

The results of the analysis of the UV and optical spectra of magnetic B stars are summarized in the Table 6. There is a discrepancy in modelling the C IV and N V doublets versus the Si IV doublet, therefore we determine the mass-loss rates in our programme stars only to within a factor of a few.

The C IV, N V and Si IV doublets differ in their sensitivity to stellar atmosphere parameters. Our models show that C IV can be the leading ionization stage in the hottest stars in our sample, such as τ Sco and ξ^1 CMa. Then X-rays destroy C IV by photoionization (see Fig. 6). (In the context of dwarf O-stars this was discussed by Martins et al. 2005; Marcolino et al. 2009). In cooler stars with $T_{\rm eff} < 27$ kK, the leading ionization stage of carbon in the wind becomes C III. In this case Auger ionization by X-rays leads to the creation of C V, followed by recombination to C IV. Therefore, the C IV line is quite sensitive both to the stellar radiation field as determined by $T_{\rm eff}$ and to the X-ray emission.

N V is not produced in the winds of stars with $T_* < 50$ kK (see fig. 3 in Hamann & Gräfener 2004). All the stars in our sample are significantly cooler, therefore the N V line in their winds originates exclusively from the ionization by X-rays. For stellar temperatures below 27 kK, the leading ion in the wind is N III, which is Auger ionized by X-rays to N V. At 27 kK and above, the leading ion is N IV. When X-rays are present in the wind, the leading ion becomes N V, or for τ Sco ($T_* = 31$ kK) even N VI.

All models that include X-ray emission and have appreciable mass-loss rates show N V with a strong P Cygni line profile, which is not observed (see Figs 11 and 21). To achieve agreement with the observations, low mass-loss rates must be adopted. For the β Cep-type variables among out programme stars, the models reproduce the observed N V doublet best if the X-ray emission is 'switched off'. Since X-ray emission is observed, one potential explanation for curiosity could be to assume some form of shielding of the cool stellar wind from the X-ray radiation.

The ionization of Si is also sensitive to stellar and X-ray radiative fields. Models predict that in the stars with $T_* < 27$ kK, the leading ion would be Si IV, but the presence of X-rays make Si V the dominant ion. Interestingly in hotter stars with photospheric temperatures above 27 kK, the dominant ion is Si V with or without X-rays; the X-rays are not sufficient to produce a significant amount of Si VI. Let us consider β Cep and τ Sco as examples. Ignoring X-ray emission in the models, Si IV is the dominant ion in the outer wind zone, and therefore the Si IV doublet becomes asymmetric in shape. With X-rays most of the Si IV in the outer wind is destroyed (ionized to Si V), and the remaining Si IV absorption is only photospheric. On the other hand in τ Sco that is hotter, the dominant ionization stage is Si V and the Si IV line is not sensitive to the X-ray emission.

These considerations show that the stellar radiation field and the X-ray emission have to be well known to use the UV lines as mass-loss rate diagnostics. There are several factors that can influence mass-loss rate determinations, and it is worth noting these and their relative importance as briefly discussed below.

Table 6. Stellar and wind parameters of τ Sco, β Cep, V2052 Oph, ξ^1 CMaand ζ Cas. The highest and the lowest mass-loss rates $\dot{M}$ as obtained from the modelling of C IV and Si IV doublets for each star are given. The $\dot{M}$ value for ξ^1 CMa is as obtained from the model of the Si IV doublet only (see Section 5.4 for details). The work ratio Q (see equation 2 for definition) is computed for the highest mass-loss rate that is given in this table.

Star	$E(B-V)$	$T_{\rm eff}$ (kK)	$\log L$ ($L_\odot$)	$\log g$ (cm s^{-2})	R ($R_\odot$)	$\log \dot{M}$ ($M_\odot$ yr^{-1})		v_∞ (km s^{-1})	$v_{\rm esc}$ (km s^{-1})	Work ratio Q	$\log\left(\frac{L_{\rm X}}{L_{\rm bol}}\right)$
						C IV	Si IV				
τ Sco	0.03	30.7	4.3	3.97	5.0	−9.3	−8.6	1000	810	2	−6.4
β Cep	0.03	25.1	4.2	3.62	7.0	−9.4	−9.1	700	640	3	−7.0
ξ^1 CMa	0.04	27.0	4.5	3.7	8.2		−10	700	750	14	−6.6
V2052 Oph	0.26	23.0	3.9	4.0	5.7	−10.7	−9.7	700	900	3	−8.0
ζ Cas	0.04	20.9	3.7	3.7	5.4	−11.0	−9.7	700	620	2	−7.5

Although the stellar radiation field is well described by our models (see Fig. 4), the detailed photospheric models (e.g. Morel & Butler 2008; Morel et al. 2008) give temperatures with uncertainties of several thousand Kelvin. Our models show that such differences in temperature are sufficient to alter the ionization stratification significantly. Thus, uncertainties in $T_{\rm eff}$ are a source of uncertainty in $\dot{M}$.

For our models we adopted abundances as derived by Morel et al. (2008). The uncertainty in abundances would reflect on the mass-loss rate determinations. However, we determine mass-loss rates only within a factor of a few, which is a higher uncertainty than could be explained by the abundances.

Another source of uncertainty is represented by the spectral and spatial specifics of the X-ray radiation. From observations we constrain the X-ray flux quite well; however, the X-ray spectral distribution is only roughly known for our sources, especially for the X-ray fainter stars (see Table 3). In addition, the location of the X-ray plasma throughout the wind is unclear.

Similar to other non-LTE stellar atmosphere models, the PoWR model assumes that the statistical equilibrium is established locally. In a situation when the densities and the wind flow times are small, the time-scale for recombinations can become longer than the time-scale for transport by advection. In their studies of low-density winds, Martins et al. (2005) tested the effects of advection and adiabatic cooling on the ionization structure and the UV lines for a star with $\log \dot{M} \approx -9$. They found that the inclusion of these effects would result in an increase in the empirically derived $\log \dot{M}$ by $\sim$0.15. This is within the error margin of the $\dot{M}$ derived for our sample stars. It is also important to note that our final results are based on unclumped wind models. If the winds are clumped, the recombination time-scale in dense clumps becomes shorter. As a test we calculated a grid of models that account for microclumping for β Cep. However, no significant difference was found compared to the unclumped models. Moreover, in our models, the N v and C v produced via Auger ionization are the leading ionization stages, therefore our assumption of local ionization balance does not introduce a large error in the model ionization structure.

We assume spherically symmetric winds. Except τ Sco which has a complex magnetic topology, the stars in our sample are oblique magnetic rotators. Their winds are likely confined by magnetic fields, therefore, the treatment by the spherically symmetric models can be a source of uncertainty.

Four of our programme stars are β Cep-type stars. As noticed by Donati et al. (2001), in principle, the mass-loss rate may change by $\approx$20 per cent in response to the $\approx$9 per cent pulsation-induced luminosity changes, while the terminal velocity should remain roughly constant. However, these changes in the $\dot{M}$ are within the errors of our estimates.

Ultimately, it appears that better determinations of the effective photospheric temperature along with a better understanding of the flow structure and X-ray sources in the systems will be needed to obtain consistent mass-loss rates that result in self-consistent fits for all of the UV wind lines.

6.8 The weak wind problem

It is known that O-type dwarfs with luminosities $\log L/{\rm L}_\odot \lesssim 5.2$ have mass-loss rates that are orders of magnitude lower than predicted by the CAK theory [see Marcolino et al. (2009) and references therein]. This discrepancy is commonly refereed to as 'the weak-wind problem'.

Babel (1996) refined the CAK theory for the B-type stars by studying the theoretical effects of shadowing by photospheric lines on radiative acceleration. It was shown that these effects have large consequences for the winds of main-sequence B stars. In particular, the main difference from the predictions of the CAK theory is found for stars with $T_{\rm eff} \approx 20\,000$–$23\,000$ K and $\log g \approx 3.7$–4.0. For these objects, the mass-loss rate is found to be lower than predicted by the CAK theory by at least a factor of 4. Among the stars in our sample, ζ Cas has values of $T_{\rm eff}$ and $\log g$ for which the theoretical wind models were computed by Babel (1996). The predicted mass-loss rate for this star is $10^{-8.8}\,{\rm M}_\odot\,{\rm yr}^{-1}$ with a terminal wind velocity of $v_\infty = 3.4 v_{\rm esc}$ (compared to $\log \dot{M} = -8.2$, $v_\infty = 1.8 v_{\rm esc}$ as predicted by the CAK theory).

Our results show that the mass-loss rate in ζ Cas does not exceed $10^{-9.7}\,{\rm M}_\odot\,{\rm yr}^{-1}$. This is $\approx$8 times smaller that the prediction of Babel (1996). Furthermore, we do not find any evidence for the predicted fast wind velocity of $v_\infty = 2100\,{\rm km\,s}^{-1}$. Similarly, for all other stars in our sample, the mass-loss rates are an order of magnitude lower than predictions by Abbott (1982) based on the CAK theory. The discrepancy with the predictions of Vink, de Koter & Lamers (2000) is even larger. Thus we conclude that all the stars in our sample belong to the category of weak-wind stars.[2]

This conclusion is corroborated by the high *work ratio* Q we find in our programme stars (see Table 6). As the work ratio Q we define the mechanical work per unit time done by the radiation field compared to the mechanical luminosity of the wind. The exact definition of Q as computed in the PoWR code is

$$Q \equiv \frac{\int_r \left[g_{\rm rad}(r) - \frac{1}{\rho(r)} \frac{{\rm d}P_{\rm g}}{{\rm d}r} \right] {\rm d}r}{\int_r \left[v \frac{{\rm d}v}{{\rm d}r} + \frac{GM_*}{r^2} \right] {\rm d}r}, \qquad (2)$$

where $g_{\rm rad}$ is the radiative acceleration, $P_{\rm g}$ is the gas pressure, and other symbols have their usual meanings. In a hydrodynamically consistent model Q equals unity. When $Q > 1$ the model predicts that there is sufficient line opacity to produce a radiative acceleration that is capable of driving a stronger wind than that observed from the UV resonant doublets. We calculated hydrodynamically consistent models by choosing $\dot{M}$ values that yield work ratios of $Q \approx 1$. Such models yield $\log \dot{M}(Q \approx 1) = -9.4$ for V2052 Oph and $\log \dot{M}(Q \approx 1) = -8.2$ for ξ^1 CMa.

Importantly, these work ratios Q are calculated from models that include X-ray emission in the ionization balance. Drew, Hoare & Denby (1994) highlighted the effect that X-ray emission may have on the wind velocity and mass-loss rate. They suggest that ionization by X-rays may change the ionization structure in the inner part of the wind, thus reducing the total radiative acceleration and consequently the mass-loss rate. Our models include the ionization by X-rays in the wind acceleration zone at the level and temperatures indicated by the X-ray observations. Yet, we find that there is still a sufficient radiative acceleration to drive mass-loss in excess of the value inferred from the UV line-fitting analysis. Therefore, the ionization by X-rays cannot be the unique solution of the weak-wind problem.

Cassinelli et al. (1994), Cassinelli (1994) and Cohen, Cassinelli & Macfarlane (1997) studied the X-ray emission from near-main-sequence B-type stars based on *ROSAT* data. They found that these stars show departure from the $L_{\rm X} \approx 10^{-7} L_{\rm bol}$ law which holds

[2] Recently Lucy (2010) identified a weak-wind domain on a $\log g$–$\log T_{\rm eff}$ diagram where a star's rate of mass-loss by a radiatively driven wind is less than that due to nuclear burning. All our programme stars belong to this domain.

for O-type stars. From evaluating the emission measure of X-ray emitting gas, they concluded that a major fraction of the wind emission measure is hot, whereas in the shocked-wind theory less than 10 per cent of the wind emission measure should be hot.

Our observations and models support these conclusions. The models show that the Emission Measure 'filling factor' of the hot material (as determined from X-ray observations) relative to the cool wind $X_{\rm fill}$ exceed unity for all our stars. While $X_{\rm fill} \approx 8$ for τ Sco is the smallest, it is as large as $X_{\rm fill} \approx 200$ for ζ Cas and extremely large $X_{\rm fill} \approx 1000$ for ξ^1 CMa. Thus, not only are the UV lines in ξ^1 CMa the most difficult to reproduce from the models, its X-ray filling factor and wind work ratio Q are also outstandingly high.

The high X-ray filling factors imply that either the hot gas $\mathrm{EM_{hot}}$ occupies a much larger volume than the cool wind $\mathrm{EM_{cool}}$ where the UV lines are formed, or that the X-ray emitting gas has a higher density. Both possibilities seem plausible in the case of magnetic stars. The cool wind can occupy a relatively smaller volume because it emerges primarily from the magnetic polar regions in stars with dipole fields. On the other hand, high-density hot plasma can occur in magnetically confined wind zones or loops.

7 DISCUSSION

7.1 X-ray emission from magnetic early-type B stars

One of the results of our study is that X-ray properties of newly discovered magnetic B-type stars are diverse. Except for τ Sco and ξ^1 CMa, our programme stars are not especially X-ray luminous. On the contrary, V2052 Oph and ζ Cas are intrinsically X-ray faint. Can these differences in luminosity be explained in the framework of the MCWS model? Babel & Montmerle (1997b) obtained a simple scaling relation between X-ray luminosity and the magnetic and stellar wind parameters in the framework of their MCWS model. They predicted that the X-ray luminosity scales approximately with the product of wind momentum and some power of the magnetic field strength, $L_{\rm X} \propto B^{0.4}\dot{M}v_\infty$ (see their equations 10– 11). We apply this scaling relation to predict X-ray luminosities for our sample stars with dipole magnetic fields. Among our sample stars, ξ^1 CMa has the strongest magnetic field, while its wind momentum is comparable to other stars. The scaling relation of Babel & Montmerle (1997b) predicts a rather weak dependence on the magnetic field strength. The predicted value of $L_{\rm X}$ (4×10^{30} erg s^{-1}) is an order of magnitude lower than the observed value. On the other hand, V2052 Oph and ζ Cas have a low wind kinetic energy and a weak magnetic field. Using the lower values of $\dot{M}$ from Table 6, the predicted X-ray luminosities for these stars ($\approx$few $\times 10^{29}$ erg s^{-1}) agree well with the observed ones. Similarly, for the lower value of $\dot{M}$ for β Cep, the predicted and observed luminosities agree quite well. Thus, the basic scalings obtained by Babel & Montmerle (1997b) for the X-ray luminosity can qualitatively explain the difference in the level of X-ray luminosity among β Cep, V2052 Oph and ζ Cas. Note, however, that using the upper values for $\dot{M}$ for these stars in the Babel & Montmerle (1997b) scaling relation would result in X-ray luminosities that are too high compared to the observed ones.

The more serious challenge is to explain the comparatively low temperatures of X-ray emitting plasma obtained from the analyses of the observed spectra, and the lack of time modulations of the X-ray flux. The X-ray spectral temperatures of magnetic B stars in our sample are not especially high. ζ Cas has one of the softest X-ray spectra among those measured in OB stars. Moreover, X-ray emissions from both τ Sco and β Cep were monitored throughout a rotation period, and neither displays rotational modulations in their X-ray light curves (Favata et al. 2009; Ignace et al. 2010).

Compared to non-magnetic stars, harder X-ray spectrum and rotationally modulated X-ray variability are predicted by *different* models of hot plasma production in magnetically confined winds (e.g. Gagné et al. 2005; Li et al. 2008). Can these models, which assume that wind motion is governed by the magnetic field, be applied to our programme stars?

It is usual to describe the relative importance of magnetic fields in gases by the plasma-β parameter with $\beta_{\rm p} = 8\pi p/B^2$, where p is the gas pressure. The gas is magnetically dominated when $\beta_{\rm p} < 1$.

For supersonic flows such as stellar winds, the ram pressure exceeds the gas pressure and the dynamical importance of a magnetic field is defined by the ratio of wind kinetic to magnetic energy density, given by the supersonic flow β viz. $4\pi\rho v^2/B^2$, where v is the supersonic flow speed. A small or large value indicates whether the magnetic field locally dominates the bulk motion, or vice versa. Supersonic rotation can be treated similarly (e.g. Brown et al 2008). Specifically, Altschuler & Newkirk (1969, and references therein) show that beyond the *Alfvén* radius $R_{\rm A}$, where

$$B^2/8\pi = \rho v^2/2 \tag{3}$$

is met, the radial stellar wind forces the magnetic field lines to become approximately radial. In contrast for $R < R_{\rm A}$, the wind flow is confined by the magnetic field.

In the context of stellar winds, wind confinement was considered by Babel & Montmerle (1997a,b), ud-Doula & Owocki (2002), Brown et al (2008) and others. Recalling that the wind density $\rho = \dot{M}/4\pi v(R)R^2$, one can express $R_{\rm A}$ from the condition set by equation (3):

$$R_{\rm A} = \sqrt{\frac{\dot{M}v(R)}{B^2}}. \tag{4}$$

In case of a dipole magnetic field $B = B_0(R_*/R)^3$, equation (4) can be rewritten as

$$r_{\rm A} \times\ w(r)^{1/4} = \left(\frac{R_*^2 B^2}{\dot{M}v_\infty}\right)^{1/4} \equiv \eta_*^{1/4}, \tag{5}$$

where $r = R/R_*$, and the standard parametric wind velocity law with $v(r) = v_\infty(1 - r^{-1})^\beta \equiv v_\infty w(r)$ is assumed. It is convenient to express η_* in terms of normalized stellar wind parameters, with $\dot{M}_{-9}$ the mass-loss rate in the units of $10^{-9}\mathrm{M}_\odot$ yr^{-1}, v_∞ in km s^{-1} and $\mathcal{R}_*$ the radius in the units of solar radius $R_\odot$. Then

$$\eta_* \approx 1 \times\ \frac{\mathcal{R}_*^2}{\dot{M}_{-9}v_\infty} \times\ B_0^2. \tag{6}$$

For stars with dipole fields (i.e. excluding τ Sco) the field strength at the magnetic pole is shown in Table 6. To estimate $r_{\rm A}$ we use as a characteristic value of the field strength at the magnetic equator (i.e. half of the polar field strength). Then we find $\eta_*(\beta\ \mathrm{Cep}) \gtrsim 3 \times 10^3$, $\eta_*(\xi^1\ \mathrm{CMa}) \approx 6 \times 10^6$, $\eta_*(\mathrm{V2052\ Oph}) \gtrsim 4 \times 10^3$ and $\eta_*(\zeta\ \mathrm{Cas}) \gtrsim 6 \times 10^3$. Consequently, the Alfvén radius is at $\approx 50\,R_*$ for ξ^1 CMa and $\lesssim 10\,R_*$ for other stars. These estimates are based on the highest mass-loss rates obtained from fitting of the UV lines.

However, we know that a significant fraction of the wind mass-loss can be in the form of hot X-ray emitting plasma. We may hypothesize that the 'true' total amount of matter is much higher. We calculated a hydrodynamically consistent model for V2052 Oph and ξ^1 CMa (see Section 6.8) to obtain a mass-loss rate of $\log \dot{M}(Q \approx 1) = -9.4$ for the former and $\log \dot{M}(Q \approx 1) = -8.2$ for the latter. Even with these higher mass-loss rates, the magnetic

fields regulate the wind motion up to $\approx 7\,R_*$ for V2052 Oph and $\approx 20\,R_*$ for ξ^1 CMa.

Thus the winds of our sample stars are strongly confined out to several stellar radii where the wind velocity should reach its terminal value. Due to the very weak signatures of the winds seen in the UV line profiles, we can establish v_∞ only with a limited degree of accuracy. Using $v_\infty \approx 700\,\mathrm{km\,s^{-1}}$ is reasonably consistent with the UV lines. Colliding wind streams at such a speed from two opposite directions of the magnetosphere should produce strong shocks, heating plasma up to ≈ 20 MK. This is far above the maximum temperatures we infer from the spectral analysis (see Table 3).

From the UV line modelling, we cannot exclude somewhat lower v_∞ for the winds of our stars, which would alleviate the expectation of very hot temperatures, scaling as v_∞^2. However, there is, perhaps, a more severe problem of the differential emission measure (DEM) distribution. The emission measure of the hottest plasma is ≈ 35 per cent of the total EM in ξ^1 CMa and only ≈ 10 per cent in β Cep. On the other hand, the plasma with the largest emission measure has a temperature of only about 1.3 MK in ξ^1 CMa (see Table 3). This dominant contribution to the DEM from the cooler hot gas component is in apparent contradiction with the predictions of the MCWS models, where the DEM is expected to peak at the hottest temperature (e.g. see fig. 8 in Nazé et al. 2010).

What could be the source of wind heating in magnetic β Cep-type stars? As pointed out by Favata et al. (2009), the relatively low temperature of the X-ray emitting plasma and the absence of flares make heating due to magnetic reconnection in analogy to active cool stars rather implausible. Heating by wind shocks owing to the intrinsic LDI mechanism in radiatively driven winds is a possibility. However, the LDI needs further theoretical studies in relation to its operation in complex geometries and the dynamics of magnetically confined winds.

Another possibility could be heating by the deposition of mechanical energy related to stellar pulsations. Cassinelli et al. (1996) found from *EUVE* observations that the β Cep-type star β CMa has an extreme ultraviolet exceeding atmosphere model predictions by an order of magnitude.[3] They suggest that this may be related to the presence of heated regions near the stellar surface owing to pulsations and magnetic fields. If the upper atmosphere is heated mechanically by pulsational effects, it is likely that the X-ray source regions are also heated by a related mechanism. In this case, the dynamic time-scale of the wind is smaller than the time required to establish ionization equilibrium.

To investigate this possibility, we show in Fig. 23 the X-ray luminosities versus pulsation periods and amplitudes for a few prominent β Cep-type variables. Given the small sample it is difficult to draw any conclusions, yet there is no apparent dependence of the X-ray luminosity on the period or pulsational amplitude.

7.2 Comparison of X-ray properties between B stars with and without confirmed magnetic fields

In this section we compare the X-ray properties of 'normal' early-type B stars where magnetic fields have not been detected up to now. The *XMM–Newton* spectrum of the β Cep-type variable β Cen (B1III) is well fitted with a three-temperature spectral model, with the hottest component $kT_{\max} \approx 0.6$ keV and $\langle kT \rangle = 0.3$ keV (Raassen et al. 2005). Hubrig et al. (2006) and Silvester et al. (2009)

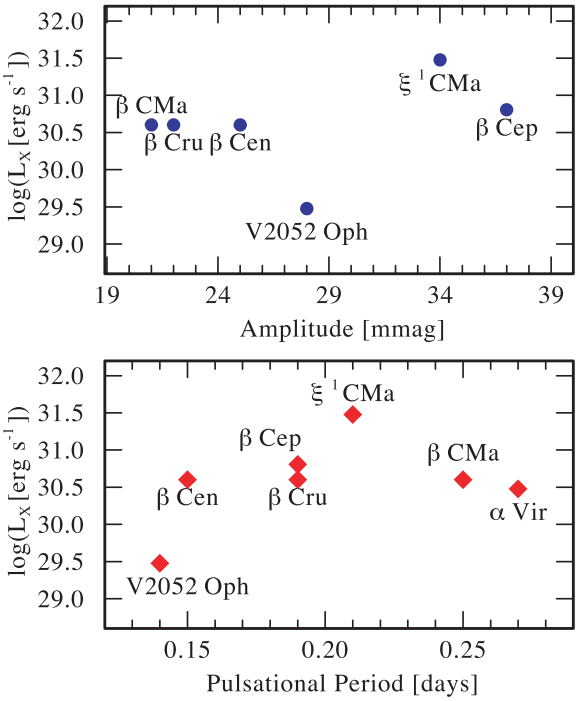

Figure 23. X-ray luminosity of some prominent β Cep-type stars versus magnitude of pulsation (upper panel) and pulsational period (lower panel) from the catalogue of Stankov & Handler (2005).

searched for a magnetic field in the β Cep-type β CMa (B1II-III) and did not detect magnetism, with errors on a longitudinal field of just 10 G. β CMa was observed by *XMM–Newton*, its spectrum is well described by a multitemperature model with the hottest temperature component at $kT = 0.3$ keV (Waldron et al., in preparation). The *Chandra* LETGS spectrum of α Vir (B1III-IV) was analysed in Zhekov & Palla (2007), who report the maximum of the emission measure distribution as being between 0.2 and 0.3 keV. We obtained the LETGS *Chandra* observations of α Cru (B0.5IV). Its X-ray temperature and luminosity are similar to those of α Vir (Ignace et al., in preparation). β Cru is another B1 giant observed by *Chandra*. Zhekov & Palla (2007) find the maximum of the emission measure distribution in this β Cep-type variable to be between 0.2 and 0.3 keV. Thus, it appears that X-ray luminosities and temperatures are very similar among the β Cep-type stars.

On the other hand, the X-ray luminosities of magnetic stars have a much greater dispersion, with two significant outliers: the X-ray luminous ξ^1 CMa and the X-ray faint V2052 Oph, while their spectral X-ray temperatures are rather similar (see Table 3). Due to the small number of stars included in our investigation, this conclusion is only preliminary. Larger samples need to be considered to draw firm conclusions about the differences in X-ray properties of magnetic and 'normal' early-type B stars.

Overall, it has emerged from our analysis that high X-ray luminosity and hard X-ray spectra are not necessary observational characteristics of the magnetic early-type stars. This conclusion fully confirms the earlier results based on the RASS data (see also recent results on X-rays from A0p stars (Robrade & Schmitt 2011).

One of the complications in massive early-type star studies is that a significant fraction of such stars is in binary or multiple systems and may have spatially unresolved companions that are intrinsic X-ray sources. An X-ray source could be spatially coincident with a B star due to a lower mass companion (Czesla & Schmitt 2007;

[3] It is possible that this problem can be resolved by a better description of X-ray emission in model atmospheres (Hamann et al., in preparation).

Remage Evans et al. 2011). In this paper we consider B0–B2 type stars. These stars are young, not older that a few 10 Myr. Possible low-mass companions would be coronally active with X-ray luminosities of 10^{28}–10^{30} erg s^{-1} (e.g. Flaccomio et al. 2003). Two newly X-ray detected stars considered in this paper, V2052 Oph and ζ Cas, have X-ray luminosities in this range (see Table 4). Therefore, in principle, we cannot rule out a confusion with an unseen coronal component. Nevertheless, we have obtained strong indications that the observed X-ray emission is intrinsic to the early-type B stars. The spectra of X-ray emission from ζ Cas and V2052 Oph are soft, e.g. in ζ Cas the average temperature is 1 MK. This is not usual for young T Tau type stars, which have average temperatures in the range of 5–30 MK (Güdel & Nazé 2009). The temperature of the X-ray emitting plasma in V2052 Oph is similar to other β Cep-type stars, albeit its X-ray luminosity is quite low (see Fig. 23). From the analysis of the UV spectra of our programme stars, we know that X-rays are present in the winds since they are required to enhance the fraction of C IV and N V in the winds (see Section 6.5). On this basis, we believe that the observed X-ray emission is intrinsic to β Cep, V2052 Oph, ζ Cas and ξ^1 CMa. Among stars in our sample, β Cep is a known binary star with a late Be-type companion. Late Be stars are not known to be intrinsic X-ray sources, therefore it seems reasonable to assume that the observed X-ray emission is intrinsic to the B2 component.

7.3 X-rays in stars with very small $\dot{M}$

ζ Cas displays quite a soft X-ray spectrum with nearly 85 per cent of the EM at temperature $\lesssim$1 MK (Fig. 3 and Table 3). Our estimate of its mass-loss rate ($\dot{M} \sim 10^{-11}$) places this object in the regime where the winds may display unusual properties.

Springmann & Pauldrach (1992) demonstrated that the assumption of a one-component fluid is not valid for low-density winds. Instead, the metal ions lose their dynamical coupling to the ions of hydrogen and helium, the bulk mass of the gas. The metal ions will move with high velocities, without helium and hydrogen being dragged along. The collisionally induced momentum transfer is accompanied by frictional heating, which dominates the energy balance. As a result, Springmann & Pauldrach (1992) predict electron temperatures of $T \sim 1$ MK in the outer wind regions for stars with mass-loss rates of $\approx 10^{-8-9}$ M$_\odot$ yr^{-1}. The subsequent analysis by Krtička & Kubát (2000) and Owocki & Puls (2002) favoured even weaker winds with $\dot{M} \sim 10^{-11}$ M$_\odot$ yr^{-1} for the wind decoupling to occur.

The theoretical analysis of this problem is not settled (e.g. Votruba et al. 2007). Gayley & Owocki (1994) investigated the effects of 'Doppler heating' in stars with low mass-loss rates, and confirmed the conclusions of Springmann & Pauldrach (1992). They also noticed that Doppler heating may lead to an instability, possibly resulting in a larger degree of microturbulence. This is an interesting prediction since our analysis favours large microturbulent broadening, as in the case of ξ^1 CMa.

Given its small $\dot{M}$ value and very soft X-ray spectrum, it is tempting to suggest that ζ Cas may be a candidate object for wind decoupling.

Another interesting mechanism for generating X-ray emission in rotating magnetic stars was put forward by Suzuki et al. (2006). They proposed that extended X-ray-emitting regions can exist in massive stars with thin winds owing to collisionless damping of fast MHD waves. Stellar rotation causes magnetic field lines anchored at the stellar surface to form a spiral pattern, and magnetorotational winds can be driven (e.g. Weber & Davis 1967). If the structure is magnetically dominated, fast MHD waves generated at the surface can propagate almost radially outwards and cross the field lines. The propagating waves undergo collisionless damping owing to interactions with particles surfing on magnetic mirrors that are formed by the waves themselves. The dissipation of the wave energy produces heating and acceleration of the outflow. The Suzuki et al. (2006) mechanism works effectively in moderate and fast rotating stars. Considering fig. 6 of Suzuki et al. (2006), the magnetic field strength, wind density and rotation speed in ζ Cas are such that the star may be in the domain where the Suzuki et al. mechanism is operational.

7.4 On the multiphase structure of winds from magnetic early B-type stars

We try to understand whether some of the facts that have emerged from our analysis can be qualitatively explained by a picture of an oblique magnetic rotator where the bulk of the stellar wind is governed by the dipole magnetic field.

Despite relatively strong surface fields, oblique magnetic rotators have open field regions near their magnetic poles, and thus may have sectors of wind flow that are similar to normal B-type stars. The UV spectra could originate in these cool sectors of the wind with a smaller filling factor as compared to the hot gas. The wind distribution is clearly asymmetric (not even axisymmetric owing to rotation). Perhaps this could explain the strange properties of the UV lines seen in ξ^1 CMa that we view nearly rotational pole-on, and possibly the large dispersion in X-ray luminosities among our sample stars as well.

The hot part of the wind is apparently heated up to a few MK. This matter is confined by the magnetic field up to $10\,R_*$, so it occupies a large volume, and, in parts, may have a high density. This would explain the large filling factors of hot material we infer from our models. The spatial separation between hot and cool gas may explain how the observed N V doublet can be weaker than predicted by our stellar atmosphere models. The total amount of matter in the cool and hot wind components may be close to values predicted by our hydrodynamically consistent models, and so the 'true' mass-loss rates are a factor of a few higher than obtained from the empirical fits of UV lines using a model that relies on spherical symmetry.

8 SUMMARY OF RESULTS

Dedicated *XMM–Newton* observations were obtained for three early-type magnetic B-type stars, ξ^1 CMa, V2052 Oph and ζ Cas. We report first detections of X-ray emission from V2052 Oph and ζ Cas. The observations show that the low-resolution X-ray spectra of our programme stars are well described by a multitemperature CIE plasma. The bulk of the emission measure originates from the plasma with a temperature of $\approx$1 MK. The X-ray luminosities differ by large factors, with ξ^1 CMa being the most X-ray luminous star in our sample, and V2052 Oph the least luminous.

We compare X-ray properties of β Cep-type variables that have magnetic field detections against those without such detections. Our comparison indicates that the general X-ray properties are quite similar, although the magnetic stars display a greater dispersion in their X-ray luminosities. Larger samples need to be studied to draw firm conclusions.

The basic MCWS model scaling relation between X-ray luminosity and stellar magnetic field and wind parameters (Babel &

Montmerle 1997b) qualitatively describes the difference in the observed level of X-ray emission from our sample stars. We searched for correlations between X-ray emission and pulsational and rotational properties of the stars but were not able to find any.

We compiled a sample of peculiar early B-type magnetic stars and considered their X-ray properties based on archival data. The comparison shows that these stars, despite very similar stellar and magnetic field parameters, have quite different X-ray properties: while some stars are hard and luminous X-ray emitters, others are apparently soft and rather faint. This new data confirm earlier results based on studies of Ap–Bp stars using the RASS data.

We analysed the spectra of five non-supergiant B stars with magnetic fields by means of the non-LTE comprehensive stellar atmosphere code PoWR. The PoWR models accurately fit the stellar photospheric spectra and also accurately reproduce the SED from the UV to the IR band.

The PoWR code was used to empirically obtain the wind parameters of τ Sco, β Cep, ξ^1 CMa, V2052 Oph and ζ Cas from the analysis of C IV, N V and Si IV doublets in stellar UV spectra.

The model UV lines depend sensitively on the parameters of X-ray emission, wind velocity and mass-loss rate. X-ray properties as derived from the observed spectra were incorporated into the wind models. We confirm that the emission measure filling factors of X-ray emitting material are high, exceeding unity for all stars.

Our analysis revealed the weak wind problem for the magnetic early-type B stars. The wind terminal speeds are of the order of stellar escape speed. The inferred mass-loss rates from the UV line analyses are significantly lower than that theoretically expected and predicted by hydrodynamically consistent wind models.

Although X-rays strongly impact the ionization structure in the wind, their effect does not reduce the total radiative acceleration enough to explain the low mass-loss rates deduced from modelling the UV lines. When X-rays at the observed level and temperatures are included in the model, there is still sufficient radiative acceleration to drive a stronger mass-loss than the observed one.

ACKNOWLEDGMENTS

This work is based on observations obtained with *XMM–Newton*, an ESA science mission with instruments and contributions directly funded by ESA Member States and NASA. We are grateful to Nolan Walborn for his comments on the manuscript and his advice on the spectral classification of our sample stars. We are also indebted to the referee, Stephen A. Drake, for very useful comments that helped to improve the clarity of the paper, and for pointing out some aspects in the studies of magnetic stars that we did not consider in the original manuscript. This research has made use of NASA's Astrophysics Data System Service and the SIMBAD data base, operated at CDS, Strasbourg, France. Funding for this research has been provided by NASA grant NNX08AW84G (RI), DLR grant 50 OR 0804 (LMO) and a UK STFC Grant (JCB).

REFERENCES

Abbott D. C., 1982, ApJ, 259, 282
Abt H. A., Levato H., Grosso M., 2002, ApJ, 573, 359
Altschuler M. D., Newkirk G., 1969, Sol. Phys., 9, 131
Arnaud K. A., 1996, in Jacoby G. H., Barnes J., eds, ASP Conf. Ser. Vol. 101, Astronomical Data Analysis Software and Systems V. Astron. Soc. Pac., San Francisco, p. 17
Asplund M., Grevesse N., Sauval A. J., Scott P., 2009, ARA&A, 47, 481
Babel J., 1996, A&A, 309, 867
Babel J., Montmerle T., 1997a, ApJ, 485, L29
Babel J., Montmerle T., 1997b, A&A, 323, 121
Baum E., Hamann W.-R., Koesterke L., Wessolowski U., 1992, A&A, 266, 402
Bohlender D. A., Landstreet J. D., Brown D. N., Thompson I. B., 1987, ApJ, 323, 325
Borra E. F., Landstreet J. D., 1979, ApJ, 228, 809
Brown J. C., Cassinelli J. P., Maheswaran M., 2008, ApJ, 688, 1320
Bychkov V. D., Bychkova L. V., Madej J., 2003, A&A, 407, 631
Cardelli J. A., Clayton G. C., Mathis J. S., 1989, ApJ, 345, 245
Cash W., 1979, ApJ, 228, 939
Cassinelli J. P., 1994, Ap&SS, 221, 277
Cassinelli J. P., Olson G. L., 1979, ApJ, 229, 304
Cassinelli J. P., Cohen D. H., Macfarlane J. J., Sanders W. T., Welsh B. Y., 1994, ApJ, 421, 705
Cassinelli J. P. et al., 1996, ApJ, 460, 949
Cassinelli J. P., Brown J. C., Maheswaran M., Miller N. A., Telfer D. C., 2002, ApJ, 578, 951
Castor J. I., Abbott D. C., Klein R. I., 1975, ApJ, 195, 157
Cohen D. H., Cassinelli J. P., Macfarlane J. J., 1997, ApJ, 487, 867
Czesla S., Schmitt J. H. H. M., 2007, A&A, 465, 493
Donati J., Landstreet J. D., 2009, ARA&A, 47, 333
Donati J., Wade G. A., Babel J., Henrichs H. F., de Jong J. A., Harries T. J., 2001, MNRAS, 326, 1265
Donati J., Babel J., Harries T. J., Howarth I. D., Petit P., Semel M., 2002, MNRAS, 333, 55
Donati J. et al., 2006, MNRAS, 370, 629
Drake S. A., Linsky J. L., Schmitt J. H. M. M., Rosso C., 1994, ApJ, 420, 387
Drew J. E., Hoare M. G., Denby M., 1994, MNRAS, 266, 917
Dziembowski W. A., Pamiatnykh A. A., 1993, MNRAS, 262, 204
Favata F., Neiner C., Testa P., Hussain G., Sanz-Forcada J., 2009, A&A, 495, 217
Feldmeier A., Kudritzki R., Palsa R., Pauldrach A. W. A., Puls J., 1997a, A&A, 320, 899
Feldmeier A., Puls J., Pauldrach A. W. A., 1997b, A&A, 322, 878
Ferrario L., Pringle J. E., Tout C. A., Wickramasinghe D. T., 2009, MNRAS, 400, L71
Flaccomio E., Damiani F., Micela G., Sciortino S., Harnden F. R., Jr, Murray S. S., Wolk S. J., 2003, ApJ, 582, 398
Gagné M., Oksala M. E., Cohen D. H., Tonnesen S. K., ud-Doula A., Owocki S. P., Townsend R. H. D., MacFarlane J. J., 2005, ApJ, 628, 986
Gayley K. G., Owocki S. P., 1994, ApJ, 434, 684
Getman K. V. et al., 2005, ApJS, 160, 319
Gräfener G., Koesterke L., Hamann W., 2002, A&A, 387, 244
Groote D., Hunger K., 1982, A&A, 116, 64
Groote D., Schmitt J. H. M. M., 2004, A&A, 418, 235
Grunhut J. H., Wade G. A., Rivinius T., Marcolino W. L. F., Townsend R., the MiMeS Collaboration 2010, preprint (arXiv:1009.3246)
Güdel M., Nazé Y., 2009, A&AR, 17, 309
Hamann W., 1981, A&A, 100, 169
Hamann W., 2010, Ap&SS, 329, 151
Hamann W., Gräfener G., 2003, A&A, 410, 993
Hamann W., Gräfener G., 2004, A&A, 427, 697
Hamann W., Koesterke L., 1998, A&A, 333, 251
Hamann W.-R., Brown J. C., Feldmeier A., Oskinova L. M., 2001, A&A, 378, 946
Henrichs H. F. et al., 2000, in Glagolevskij Y. V., Romanyuk I. I., eds, Magnetic Fields of Chemically Peculiar and Related Stars. p. 57
Henrichs H. F., Schnerr R. S., ten Kulve E., 2005, in Ignace R., Gayley K. G., eds, ASP Conf. Ser. Vol. 337, The Nature and Evolution of Disks around Hot Stars. Astron. Soc. Pac., San Francisco, p. 114
Hillier D. J., Miller D. L., 1999, ApJ, 519, 354
Hubrig S., Briquet M., Schöller M., De Cat P., Mathys G., Aerts C., 2006, MNRAS, 369, L61
Hubrig S., Briquet M., Morel T., Schöller M., González J. F., De Cat P., 2008, A&A, 488, 287

Hubrig S., Ilyin I., Schöller M., Briquet M., Morel T., De Cat P., 2011, ApJ, 726, L5
Hunger K., Heber U., Groote D., 1989, A&A, 224, 57
Ignace R., Oskinova L. M., Jardine M., Cassinelli J. P., Cohen D. H., Donati J., Townsend R. H. D., ud-Doula A., 2010, ApJ, 721, 1412
Kaper L. et al., 1997, A&A, 327, 281
Krtička J., Kubát J., 2000, A&A, 359, 983
Leone F., 1994, A&A, 286, 486
Li Q., Cassinelli J. P., Brown J. C., Waldron W. L., Miller N. A., 2008, ApJ, 672, 1174
Liermann A., Hamann W., Oskinova L. M., Todt H., Butler K., 2010, A&A, 524, A82
Lucy L. B., 2010, A&A, 512, A33
Lucy L. B., Solomon P. M., 1970, ApJ, 159, 879
Macfarlane J. J., Cassinelli J. P., 1989, ApJ, 347, 1090
Maheswaran M., 2003, ApJ, 592, 1156
Maheswaran M., Cassinelli J. P., 2009, MNRAS, 394, 415
Marcolino W. L. F., Bouret J., Martins F., Hillier D. J., Lanz T., Escolano C., 2009, A&A, 498, 837
Martins F., Schaerer D., Hillier D. J., Meynadier F., Heydari-Malayeri M., Walborn N. R., 2005, A&A, 441, 735
Mewe R., Raassen A. J. J., Cassinelli J. P., van der Hucht K. A., Miller N. A., Güdel M., 2003, A&A, 398, 203
Morel T., Butler K., 2008, A&A, 487, 307
Morel M., Magnenat P., 1978, A&AS, 34, 477
Morel T., Hubrig S., Briquet M., 2008, A&A, 481, 453
Mullan D. J., 2009, ApJ, 702, 759
Nazé Y., 2009, A&A, 506, 1055
Nazé Y., Ud-Doula A., Spano M., Rauw G., De Becker M., Walborn N. R., 2010, A&A, 520, A59
Neiner C., Geers V. C., Henrichs H. F., Floquet M., Frémat Y., Hubert A., Preuss O., Wiersema K., 2003a, A&A, 406, 1019
Neiner C. et al., 2003b, A&A, 411, 565
Oskinova L. M., Hamann W., Feldmeier A., 2007, A&A, 476, 1331
Owocki S. P., Puls J., 2002, ApJ, 568, 965
Petit V., Wade G. A., Drissen L., Montmerle T., Alecian E., 2008, MNRAS, 387, L23
Petit V., Massa D. L., Marcolino W. L. F., Wade G. A., Ignace R., 2011, MNRAS, 412, 45
Prinja R. K., 1989, MNRAS, 241, 721
Raassen A. J. J., Cassinelli J. P., Miller N. A., Mewe R., Tepedelenlioğlu E., 2005, A&A, 437, 599
Reiners A., Stahl O., Wolf B., Kaufer A., Rivinius T., 2000, A&A, 363, 585
Remage Evans N. et al., 2011, ApJS, 194, 13
Robrade J., Schmitt J. H. M. M., 2011, A&A, 531, 58
Rogerson J. B., Jr, Upson W. L., II, 1977, ApJS, 35, 37
Romanyuk I. I., Kudryavtsev D. O., 2008, Astrophys. Bull., 63, 139
Sanz-Forcada J., Franciosini E., Pallavicini R., 2004, A&A, 421, 715
Schnerr R. S., Henrichs H. F., Oudmaijer R. D., Telting J. H., 2006, A&A, 459, L21
Schnerr R. S. et al., 2008, A&A, 483, 857
Silvester J. et al., 2009, MNRAS, 398, 1505
Simón-Díaz S., García-Rojas J., Esteban C., Stasińska G., López-Sánchez A. R., Morisset C., 2011, A&A, 530, A57
Skrutskie M. F. et al., 2006, AJ, 131, 1163
Sota A., Maíz Apellániz J., Walborn N. R., Alfaro E. J., Barbá R. H., Morrell N. I., Gamen R. C., Arias J. I., 2011, ApJS, 193, 24
Springmann U. W. E., Pauldrach A. W. A., 1992, A&A, 262, 515
Stankov A., Handler G., 2005, ApJS, 158, 193
Strüder L. et al., 2001, A&A, 365, L18
Sutherland R. S., Dopita M. A., 1993, ApJS, 88, 253
Suzuki T. K., Yan H., Lazarian A., Cassinelli J. P., 2006, ApJ, 640, 1005
Telting J. H., Aerts C., Mathias P., 1997, A&A, 322, 493
Todt H., Peña M., Hamann W., Gräfener G., 2010, A&A, 515, A83
Townsend R. H. D., Owocki S. P., Ud-Doula A., 2007, MNRAS, 382, 139
Turner M. J. L. et al., 2001, A&A, 365, L27
ud-Doula A., Owocki S. P., 2002, ApJ, 576, 413
van Leeuwen F., 2007, A&A, 474, 653
Vink J. S., de Koter A., Lamers H. J. G. L. M., 2000, A&A, 362, 295
Votruba V., Feldmeier A., Kubát J., Rätzel D., 2007, A&A, 474, 549
Walborn N. R., Fitzpatrick E. L., 1990, PASP, 102, 379
Weidner C., Vink J. S., 2010, A&A, 524, A98
Yudin R. V., 2001, A&A, 368, 912
Zhekov S. A., Palla F., 2007, MNRAS, 382, 1124

This paper has been typeset from a TEX/LATEX file prepared by the author.